LINEARIZED THEORY OF GAS-DYNAMIC-LASER
NOZZLE WAKES AND APPLICATIONS

FORD AEROSPACE AND COMMUNICATIONS CORP.
NEWPORT BEACH, CALIFORNIA

OCTOBER 1976

AERONUTRONIC FORD PUBLICATION NO. U-6276

LINEARIZED THEORY OF
GAS-DYNAMIC-LASER NOZZLE WAKES
AND APPLICATIONS

Prepared by:
Anthony Demetriades

Ford Aerospace and Communications Corp.
Aeronutronic Division
Ford Road
Newport Beach, California
92663

Sponsored by:

United States Air Force
Special Weapons Laboratory
Kirtland AFB, New Mexico

Monitored by:

Air Force Office of Scientific Research
Building 410
Bolling Air Force Base
Washington, D.C. 20332

Under Contract:

F44620-75-C-0016

October 1976

DDC

FEB 8 1977

D

Qualified requestors may obtain additional copies from the
Defense Documentation Center, all others should apply to the
National Technical Information Service

SECURITY CLASSIFICATION OF THIS PAGE *(When Data Entered)*

REPORT DOCUMENTATION PAGE	READ INSTRUCTIONS BEFORE COMPLETING FORM

1. REPORT NUMBER AFOSR - TR - 77 - 0031	2. GOVT ACCESSION NO.	3. RECIPIENT'S CATALOG NUMBER

4. TITLE *(and Subtitle)* LINEARIZED THEORY OF GAS-DYNAMIC-LASER NOZZLE WAKES AND APPLICATIONS	5. TYPE OF REPORT & PERIOD COVE..ED INTERIM
	6. PERFORMING ORG. REPORT NUMBER

7. AUTHOR(s) ANTHONY DEMETRIADES	8. CONTRACT OR GRANT NUMBER(s) F44620-75-C-0016

Ford Aerospace and Communications Corp.
Aeronutronic Division
Ford Road
Newport Beach, California.   C DIV
92663

9.	10. PROGRAM ELEMENT, PROJECT, TASK AREA & WORK UNIT NUMBERS 681307 9781-03 61102F

11. CONTROLLING OFFICE NAME AND ADDRESS AIR FORCE OFFICE OF SCIENTIFIC RESEARCH/NA BLDG 410 BOLLING AIR FORCE BASE, D C 20332	12. REPORT DATE October 1976
	13. NUMBER OF PAGES 65

14. MONITORING AGENC NAME & ADDRESS*(if different from Controlling Office)*	15. SECURITY CLASS. *(of this report)* UNCLASSIFIED
	15a. DECLASSIFICATION/DOWNGRADING SCHEDULE

16. DISTRIBUTION STATEMENT *(of this Report)*

Approved for public release; distribution unlimited.

17. DISTRIBUTION STATEMENT *(of the abstract entered in Block 20, if different from Report)*

18. SUPPLEMENTARY NOTES

19. KEY WORDS *(Continue on reverse side if necessary and identify by block number)*
LASERS
NOZZLES
WAKES
TURBULENCE
BOUNDARY LAYER

20. ABSTRACT *(Continue on reverse side if necessary and identify by block number)*
The equations describing the development of wakes trailing from gas-dynamic-laser nozzle cusps are assembled in compact form. A particular family of appropriately short, geometrically similar DeLaval nozzles are considered. The exit flow is assumed parallel and the trailing edge thickness is taken to be sharp. Fully laminar and fully turbulent wakes are considered for arbitrary exit Mach and Reynolds number, specific heat ratio and nozzle-to-stagnation temperature ratio. The total viscous drag and heat exchanged with the nozzle cusp are calculated, for such conditions, for both laminar and turbulent nozzle

DD FORM 1473 EDITION OF 1 NOV 65 IS OBSOLETE
1 JAN 73

boundary layer. To calculate the laminar wake, Kubota's linearized similarity theory is then utilized; for the turbulent wake an analogous similarity theory is used, with key information on turbulent transport drawn from recent two-dimensional supersonic wake experiments. The results are given in non-dimensional form by expressing distances in terms of the nozzle exit height. Most wake parameters are found insensitive to Reynolds number but strongly dependent on the other design parameters. Procedures are indicated and charts and tables are supplied by which the reader can apply the formulas to any set of design parameters, and a specific example at Mach 4 is computed in detail. Assumptions and approximations are pointed out for future test by experiment.

FOREWORD

This technical report is written in the course of a program entitled:
"Linearized Theory of Gas-Dynamic-Laser Nozzle Wakes and Applications,"
sponsored by AFSWC, Kirtland AFB, New Mexico and monitored by AFOSR under
Contract No. F44620-75-C-0016. This phase of the work deals with the general
subject of the flow exiting adjacent supersonic nozzles. Specifically, it is
sought to characterize and predict the development of wakes emanating from
the trailing edges of the cusps formed by such adjacent nozzles. Wake meas-
urements are carried out at the Aeronutronic Ford Supersonic Wind Tunnel
under this program; the data will then be used to test the adequacy of
theories predicting the wake development. This report summarizes the basic,
linearized flow theory predicting the development of the wake, for comparison
with the experimental data.

The author is indebted to P.J. Ortwerth of AFSWC for guidance and encourage-
ment in this work, and to Milton Rogers of AFOSR for his assistance in this
program.

ib
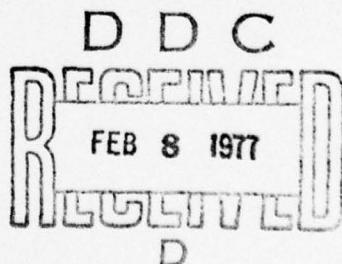
ABSTRACT

The objective of this report is to assemble, in compact form, the equations
describing the development of wakes trailing from gas-dynamic-laser nozzle
cusps. A particular family of appropriately short, geometrically similar
DeLaval nozzles are considered. The exit flow is assumed parallel and the
trailing edge thickness is taken to be sharp. Fully laminar and fully
turbulent wakes are considered for arbitrary exit Mach and Reynolds number,
specific heat ratio and nozzle-to-stagnation temperature ratio. The total
viscous drag and heat exchanged with the nozzle cusp are calculated, for
such conditions, for both laminar and turbulent nozzle boundary layer. To
calculate the laminar wake, Kubota's linearized similarity theory is then
utilized; for the turbulent wake an analogous similarity theory is used,
with key information on turbulent transport drawn from recent two-dimensional
supersonic wake experiments. The results are given in non-dimensional
form by expressing distances in terms of the nozzle exit height. Most wake
parameters are found insensitive to Reynolds number but strongly dependent
on the other design parameters. Procedures are indicated and charts and
tables are supplied by which the reader can apply the formulas to any set
of design parameters, and a specific example at Mach 4 is computed in detail.
Assumptions and approximations are pointed out for future test by experiment.

CONTENTS

CONTENTS (Continued)

LIST OF SYMBOLS

A : nozzle flow area

A' : quantity in Kubota's wake theory (see eq. (74))

B' : quantity in Kubota's wake theory (see eq. (74))

c_p : specific heat at constant pressure

c_f : skin friction coefficient

b_u : physical wake thickness (99% velocity point)

b_t : physical wake thickness (99% temperature point)

$\mathcal{b}_u$: compressible transformation of b_u

$\mathcal{b}_t$: compressible transformation of b_t

c_H : heat transfer coefficient

C_L : constant in laminar skin friction expression

C_T : constant in turbulent skin friction expression

C_n : coefficients in the nozzle contour (see eq. (17))

$c_D h$: momentum thickness of wake

d : characteristic length of theoretical wake-producing body

f : a function of Mach number (see eq. (67))

F_v : viscous force on nozzle (per unit span)

F : a function of Mach number and γ (see Table III)

$\mathcal{F}$: a function of Mach number and γ (see Table V)

G : a function of Mach number and γ (see Table X)

GDL : Gas dynamic laser

h_1 : nozzle exit height

i : a function of Mach number and γ (see Table IV)

i' : a function of Mach number and γ (see Table VI)

i'' : a function of Mach number and γ (see Table VIII)

i''' : a function of Mach number and γ (see Table XII)

J : a function of Mach number and γ (see eq. (64))

K : a function of Mach number and γ (see Table XIII)

ℓ : streamwise length from nozzle throat to trailing edge

L : wake transverse scale (eq. 104)

M : Mach number

N : a function of Mach number and γ (see Table IX)

p : pressure

q : local heat flux

$\bar{Q}$: total power flux of nozzle per unit span

Q : non-dimensional total power flux of nozzle per unit span

r : wake density defect = $(\rho_\infty - \rho(0))\rho_\infty$

Re' : unit local Reynolds number

Re : Reynolds number

Re_ξ : local Reynolds number based on distance from nozzle throat

$Re_{\infty\ell}$: Reynolds number based on nozzle exit properties and ℓ

$Re_{\infty h_1}$: Reynolds number based on nozzle exit properties and h_1

R_T : turbulent Reynolds number (a constant)

S : a function of Mach number and γ (Table VII)

t : wake static temperature defect $= (T(0) - T_\infty)/T_\infty$

T : temperature

T.E.: trailing edge of nozzle cusp

u : flow velocity

$\tilde{u}$: lateral velocity function $= (u_\infty - u)/(u_\infty - u(0))$

$\tilde{u}_u$: $\tilde{u}$ at the wake edge ($= 0.01$ herein)

w : wake velocity defect $= (u_\infty - u(0))/u_\infty$

$\tilde{T}$: lateral temperature function $= (T_\infty - T)/(T_\infty - T(0))$

$\tilde{T}_O$: lateral total temperature function $= (T_{O\infty} - T_O)/(T_{O\infty} - T_O(0))$

x : streamwise distance, positive going downstream $(x(T.E.) = 0)$

x_O : x at wake virtual origin

y : lateral distance ($y = 0$ on wake centerplane or "axis")

$\tilde{y}$: transformed lateral distance

y_t : physical distance from wake axis to wake edge

$\tilde{y}_t$: transformed distance from wake axis to wake edge

$\tilde{y}_u$: $\tilde{y}_t$

z : function of M and M_∞ (see eq. (12))

LIST OF SYMBOLS
(cont'd)

α : temperature function $= (T_w/T_o) - 1$

β : Mach number function $= 1 + (\gamma - 1) M^2/2$

γ : ratio of specific heats

Δx : streamwise distance, positive downstream ($\Delta x = 0$ at virtual origin)

η : non-dimensional lateral coordinate $= \tilde{y}/L$

θ^* : momentum thickness of nozzle boundary layer

θ^*_ζ : θ^* at nozzle trailing edge

Θ : wake total temperature defect $= (T_{o\infty} - T_o(0)/T_{o\infty}$

μ : viscosity

ξ : streamwise coordinate, positive downstream ($\xi = 0$ at nozzle throat)

ρ : density

$\tilde{\rho}$: lateral density function $= (\rho_\infty - \rho)/(\rho_\infty - \rho(0))$

σ : Prandtl number

σ_T : turbulent Prandtl number

τ_w : local friction force on nozzle wall (per unit span)

χ : lateral distance between cusp plane of symmetry and nozzle surface

$(\ )$: supply (stagnation) chamber properties (note: $T_o = T_{o\infty}$)

$(\ )^*$: conditions at nozzle throat

$(\ )_\infty$: conditions at nozzle exit

$(\ )_w$: conditions on nozzle wall

LIST OF FIGURES

I. INTRODUCTION

The technique of "stacking" supersonic DeLaval nozzles on top of one another
is at present the standard method of expanding a flowing gas to low temper-
ature supersonic flow over a short physical distance. This "nozzle array"
allows, in principle, the expansion length to be small regardless of the
mass flow, and is therefore a good scheme for high-power gas-dynamic lasers.
Ideally, uniform supersonic flow is obtained in the discharge volume (the
"laser cavity"). In practice, however, each nozzle cusp sheds a supersonic
wake which, by definition, introduces flow non-uniformity in the cavity.
Non-uniformities degrade the laser performance, and it is thus important to
predict the cusp wake flow for each given set of GDL operating conditions.

This report presents formulas describing laminar and turbulent wake behavior
for various nozzle exit Mach and Reynolds numbers, specific heat ratios and
nozzle wall temperatures. Such generality is achieved by "standardizing"
the nozzle contour and utilizing the linearized, similarity approach to wake
flow. For laminar wakes this linearized solution has been available for some
time. A corresponding solution has been available for the turbulent wake,
with the transport coefficients given from experiments on two-dimensional
supersonic wakes. The disadvantage of the linearized solution is its inval-
idity near the cusp trailing edge, and also when the design parameters lie
on certain extreme ranges. The advantage lies in the compactness with which
the results are expressed in charts and tables. Also, the qualitative trends
in wake behavior with changing parameter values should not then change much
if non-linear, exact solutions were to be found.

2. STATEMENT OF THE PROBLEM AND SUMMARY OF THE SOLUTION

The geometrical configuration of the problem is shown on Fig. 1. A nozzle
"cusp" is enclosed symmetrically by two nozzle contours. The nozzle exit
flow is parallel to the axis and the cusp T.E. (trailing edge) is taken as
infinitely thin. The nozzles are assumed perfectly two-dimensional, i.e.,
no interaction is allowed between their flow and the boundary layer growing
on the nozzle sidewall. Two-dimensionality is also assumed for the wake and
nozzle flow downstream of the T.E.

Because of momentum and heat balance, the wake integral properties are con-
trolled by what happens on the nozzle surfaces. Therefore, it is first im-
portant to "standardize" the nozzle contour, i.e., to find a family of nozzles
whose non-dimensional coordinates are functions of M_∞ alone; this is done
in Section 5. Then, Section 6 calculates the momentum and heat exchange
between nozzles and flow, as a function of M_∞, Re', γ and T_w/T_o. This cal-
culation is done both for laminar and turbulent flow (Sections 7.1 and 7.2
respectively.)

In Section 7.1, the linearized laminar wake theory of Kubota's is written
down and, with the inputs from Section 5, used to express specific variations
for the laminar wake properties. The same is done for turbulent wakes in

1

Section 7.2, except that Kubota's theory is replaced by the standard linearized turbulent wake analysis with pivotal inputs on turbulent transport coefficients taken from experiment.

Sections 7.1 and 7.2 contain all the formulas needed to predict the longitudinal and lateral variations of fluid velocity, temperature, etc., as a function of the GDL design parameters. A guide for using these formulas in step-by-step fashion is presented in Section 8.1, and a numerical example of this step-by-step process is given in Section 8.2. Finally, a complete set of computations is given in Section 8.3 for the $M_\infty = 4$, $\gamma = 1.4$ case, which is the case selected for experimental verification in the Aeronutronic Ford Supersonic Wind Tunnel.

3. ASSUMPTIONS AND APPROXIMATIONS

The following assumptions and approximations will be made:

A. The subsonic portion of the nozzle cusps contributes nothing to the total nozzle heat transfer and skin friction.

B. The friction and heat transfer coefficients at any distance ξ (measured from the throat along the nozzle axis) on the nozzle surface are equal to those at distance ξ from the leading edge of a flat plate in uniform flow, at edge conditions equal to those on the nozzle axis at ξ, and without pressure gradient.

C. The laminar friction and heat transfer coefficients are independent of the local Mach M, and of the local heat transfer rate.

D. The turbulent friction coefficient is independent of heat transfer.

E. The Prandtl number along the nozzle wall is constant.

Note that assumption (A) is especially reasonable for GDL nozzles, which are almost always designed to contract and expand the flow quickly. Fig. 1 shows typical GDL nozzle geometries.

4. GENERAL EXPRESSIONS FOR GDL NOZZLE FRICTION FORCE AND HEAT EXCHANGE

In Sections 4-6, we use the coordinate ξ to describe streamwise distance along the nozzle axis, with $\xi = 0$ at the nozzle throat (see Fig. 1). In later Sections, the coordinate x, zero at the T.E., is used in connection with the wake flow.

Since the flow is two-dimensional, the total friction force per unit span on the nozzle "cusp" (Fig. 1) is twice the integral of the shear force from the throat ($\xi = 0$) to the trailing edge (T.E.):

2

$$F_v \equiv \text{TOTAL FORCE /SPAN} = 2 \int_0^\ell \tau_w \, d\zeta \tag{1}$$

For reasons evident later, we wish to normalize F_v with the quantities at the exit nozzle:

$$\frac{F_v}{\frac{1}{2} \rho_\infty u_\infty^2} = \frac{2\ell}{\frac{1}{2} \rho_\infty u_\infty^2} \int_0^1 \tau_w \, d\left(\frac{\zeta}{\ell}\right) \tag{2}$$

Since

$$c_f \equiv \frac{\tau_w}{\frac{1}{2} \rho u^2} \tag{3}$$

we get

$$\frac{F_v}{\frac{1}{2} \rho_\infty u_\infty^2} = 2\ell \int_0^1 c_f \frac{\frac{1}{2} \rho u^2}{\frac{1}{2} \rho_\infty u_\infty^2} \, d\left(\frac{\zeta}{\ell}\right) = 2\ell \int_0^1 c_f \frac{\rho}{\rho_\infty} \frac{u^2}{u_\infty^2} \, d\left(\frac{\zeta}{\ell}\right) \tag{4}$$

or, since $\rho u^2 \sim pM^2$,

$$\frac{F_v}{\frac{1}{2} \rho_\infty u_\infty^2} = 2\ell \frac{p_0}{p_\infty} \frac{1}{M_\infty^2} \int_0^1 c_f \frac{p}{p_0} M^2 d\left(\frac{\zeta}{\ell}\right) \tag{5}$$

It can be shown that an analogous expression holds for the thermal power exchanged between the cusp and the flow:

$$\bar{Q} \equiv \text{POWER EXCHANGED /SPAN} = 2\ell \int_0^1 q_w \, d\left(\frac{\zeta}{\ell}\right) \tag{6}$$

where q_w is the power flux. Our general purpose is to reduce eq. (5) and eq. (6) in terms of non-dimensional variables such as the ratio of specific heats γ, the exit Mach number M_∞ and Reynolds number Re_∞, the Prandtl number σ_∞ and the ratio T_w/T_0 of nozzle wall to stagnation temperature. We observe that

$$\frac{p_\infty}{p_0} = \frac{p_\infty}{p_0}(M_\infty, \gamma) \tag{7}$$

3

$$c_f = c_f(M, \sigma, \gamma, Re) = c_f(M, \sigma, \gamma ; Re_\infty, M_\infty) \quad (8)$$

$$\frac{\rho}{\rho_\infty} = \frac{\rho}{\rho_\infty}(M, M_\infty, \gamma) \quad (9)$$

$$\frac{u}{u_\infty} = \frac{u}{u_\infty}(M, M_\infty, \gamma) \quad (10)$$

Since M is a function of ξ/ℓ in general, our objective is in principle attainable since, upon integration, the integral in eq. (5) or eq. (6) will only be a function of exit quantities (subscript ∞).

5. PRESCRIPTION OF THE GDL NOZZLE CONTOUR

As just mentioned, the integral in eq. (5) and eq. (6) can be integrated into an expression involving nozzle exit quantities only. For any given nozzle, the function $M = M(\xi/\ell)$ is also given, by definition. Then, the quantities in the integrand can be expressed in terms of M and thus also in terms of ξ/ℓ; for example:

$$\frac{P}{P_0} = \frac{P}{P_0}\left(M\left(\frac{\xi}{\ell}\right)\right) = \frac{P}{P_0}\left(\frac{\xi}{\ell}\right) \quad (11)$$

This procedure will be displayed in detail later, when the integrals (5) and (6) are actually computed (see Section 6.)

The above procedure, however, cannot be generalized for arbitrary nozzles of arbitrary exit M_∞, since it is well known that there is no <u>unique</u> function $M(\xi/\ell)$ for DeLaval nozzles. We wish to set as an objective the evaluation of the integrals (5) and (6) for such "general" nozzles and for arbitrary M_∞. Thus we week a function, say $z(M)$, which depends on ξ/ℓ so that M_∞ does not appear explicitly. One of the simplest choices is

$$z = z(M) = \frac{M-1}{M_\infty-1} = 0 \quad @ \; M=1 \quad (\xi/\ell = 0) \quad (12)$$

$$= 1 \quad @ \; M=M_\infty \; (\xi/\ell = 1) \quad (13)$$

4

and

$$M = z(M_\infty - 1) + 1 \qquad (14)$$

Thus, z = 0 at the nozzle throat and 1 at the nozzle exit.

Consider now, that there is a function $z(\xi/\ell)$ which is unique for all DeLaval nozzles. Then for each ξ/ℓ a z is obtained and, through eq. (14), also a M once the exit M_∞ is given. The strategy of evaluating the integral in (5) or (6) once M_∞ is given is: first, express all quantities in the integrand in terms of M, then in terms of z (using eq. (12)) and then in terms of ξ/ℓ using the known $z(\xi/\ell)$. The integral can then be evaluated, the final expression containing M_∞ (and also Re_∞, γ, etc., as they appeared in the integrand). Thus the viscous force of the nozzle cusp

$$\frac{F_v}{\frac{1}{2}\rho_\infty u_\infty^2} = fn \text{ of } (M_\infty, Re_\infty, \gamma \text{ etc.}) \qquad (15)$$

As mentioned above, there appears to be no unique function $z(\xi/\ell)$ for all nozzles. However, Shames and Seashore (Ref. 1) indicate that there exists a family of "short" supersonic nozzles, treated in their paper, which shows distinct geometric similarity for all M_∞. Such "short" nozzles are obviously suitable for GDL's. Availing ourselves of this coincidence, we make the following assumption in this work:

(F)   "The supersonic nozzles discussed here (also called "GDL" nozzles) are characterized by a unique function

$$z = z\left(\frac{\xi}{\ell}\right) = \frac{M-1}{M_\infty - 1} \qquad " \qquad (16)$$

The next step is to find $z(\xi/\ell)$. A GDL nozzle for $M_\infty = 4$ has been designed, and its M at each ξ (or ξ/ℓ) is shown on Table I. From M and M_∞ the variation of z vs ξ/ℓ was plotted on Fig. 2. This curve was next least-squares fitted by

$$z = \sum_{n=1} C_n \left(\frac{\xi}{\ell}\right)^n \qquad (17)$$

Trials were made with polynomials of degrees 4 through 8, the coefficients being shown on Table II. The 8th degree polynomial best fits the $z(\xi/\ell)$ curve, as shown on Fig. 2, but all integrals were also evaluated using lesser-degree polynomials as will be seen.

In summary, based on the coordinates of the designed $M_\infty = 4$ nozzle, the function $z = (M-1)/(M_\infty-1)$ was analytically found as a function of ξ/ℓ, by curve-fitting. It was then assumed that $z(\xi/\ell)$ was universal for GDL nozzles. This enabled the calculation of the integrals to proceed, as will now be done.

6. CALCULATION OF GDL-NOZZLE VISCOUS DRAG AND HEAT EXCHANGE

6.1 VISCOUS DRAG IN LAMINAR FLOW

To calculate $F_V/\frac{1}{2}\rho_\infty u_\infty^2$ from (5), write c_f in accordance with assumption (B) of Section 3.

$$c_f = \frac{C_L}{(Re_\zeta)^{1/2}} \quad , \quad Re_\zeta \equiv \frac{\rho u \zeta}{\mu} \tag{18}$$

which, with $C_L = 0.664$, is the well known laminar incompressible expression (Ref. 2). Then, from (5) we obtain

$$\frac{F_V}{\frac{1}{2}\rho_\infty u_\infty^2} = 2\ell \frac{P_0}{P_\infty} \frac{1}{M_\infty^2} \frac{C_L}{\sqrt{Re_{\infty\ell}}} \int_0^1 \left(\frac{\ell}{\zeta} \frac{A}{A_\infty} \frac{\mu}{\mu_\infty} \right)^{\frac{1}{2}} \frac{P}{P_0} M^2 d\left(\frac{\zeta}{\ell} \right) \tag{19}$$

where

$$A/A_\infty = \rho_\infty u_\infty / \rho u \quad , \quad Re_{\infty\ell} \equiv \rho_\infty u_\alpha \ell / \mu_\infty \quad , \text{ or}$$

$$\frac{F_V}{\frac{1}{2}\rho_\infty u_\infty^2} = 2\ell \frac{P_0}{P_\infty} \frac{1}{M_\infty^2} \frac{C_L}{\sqrt{Re_{\infty\ell}}} \left(\frac{A^*}{A_\infty} \frac{\mu_0}{\mu_\infty} \right)^{\frac{1}{2}} \int_0^1 \left(\frac{\ell}{\zeta} \frac{A}{A^*} \frac{\mu}{\mu_0} \right)^{\frac{1}{2}} \frac{P}{P_0} M^2 d\left(\frac{\zeta}{\ell} \right) \tag{20}$$

From the familiar isentropic expressions with

$$\beta \equiv 1 + \frac{\gamma-1}{2} M^2 \tag{21}$$

$$\left(\frac{A}{A^*} \right)^{1/2} = \left(\frac{\gamma+1}{2} \right)^{-\frac{\gamma+1}{4(\gamma-1)}} \frac{1}{\sqrt{M}} \beta^{\frac{\gamma+1}{4(\gamma-1)}} \tag{22}$$

$$\frac{P}{P_0} = \beta^{-\frac{\gamma}{\gamma-1}} \tag{23}$$

6

For the viscosity, we assume

$$(G) \qquad \frac{\mu}{\mu_0} = \left(\frac{T}{T_0} \right)^{0.76} \tag{24}$$

so that

$$\left(\frac{\mu}{\mu_0} \right)^{\frac{1}{2}} = \beta^{-0.38} \tag{25}$$

Combining eq. (22, (23) and (25) into (20) we get:

$$\frac{F_v}{\frac{1}{2} \rho_\infty u_\infty^2} = \left(\frac{2 l C_L}{\sqrt{Re_{\infty l}}} \right) F i = fn \left(l, Re_{\infty l}, M_\infty, \gamma \right) \tag{26}$$

where:

$$F \equiv \left(\frac{\gamma+1}{2} \right)^{-\frac{\gamma+1}{4(\gamma-1)}} \frac{P_0}{P_\infty} \frac{1}{M_\infty^2} \left(\frac{A^*}{A_\infty} \frac{\mu_0}{\mu_\infty} \right)^{\frac{1}{2}} = F(M_\infty, \gamma) \tag{27}$$

$$i \equiv \int_0^1 \left(\frac{l}{\xi} \right)^{\frac{1}{2}} M^{\frac{3}{2}} \beta^{\frac{\gamma+1}{4(\gamma-1)} - \frac{\gamma}{\gamma-1} - 0.38} d\left(\frac{\xi}{l} \right) = i(M_\infty, \gamma) \tag{28}$$

The value of F was computed for M_∞ = 2,3,4,5, and 6, and for γ = 1.2, 1.3, 1.4, 1.5, 1.6 and 1.667 at each M, and is shown on Table III. The integral i was computed numerically using the TSS NUMINT program, with M expressed as a function of (ξ/l) through eq. (12) and eq. (17). It is shown on Table IV.

It is important to relate the viscous force on the nozzle with identifiable properties of the nozzle flow. From the Karman integral equation for the momentum thickness on a plate, we get one approximate relation:

$$\tau_w \simeq \rho_\infty u_\infty^2 \frac{d\theta^*}{d\xi} \tag{29}$$

from which,

$$F_v \equiv 2 \int_0^l \tau_w d\xi = 2 \rho_\infty u_\infty^2 \theta_l^* \tag{30}$$

7

where θ_L^* is the momentum thickness on the nozzle (assumed equivalent to a flat plate) trailing edge. Inserting (30) into (26) we get

$$4\theta_l^* = \frac{F_v}{\frac{1}{2}\rho_\infty u_\infty^2} = \left(\frac{2 l C_L}{\sqrt{Re_{\infty l}}}\right) Fi \tag{31}$$

Another relation, to prove very useful later on, connects F_v with the "Momentum defect" of the wake:

(Viscous force)/span = (Momentum wake change)/span

or

$$2 \int_0^l \tau_w \, d\xi = \int_{-\infty}^{\infty} \rho u (u_\infty - u) \, dy \quad \text{(in the wake)} \tag{32}$$

When divided by $1/2\rho_\infty u_\infty^2$, the r.h.s. is the familiar momentum defect of the wake:

$$C_D h \equiv 4 \int_0^\infty \frac{\rho u}{\rho_\infty u_\infty} \left(1 - \frac{u}{u_\infty}\right) dy \tag{33}$$

from which, with the aid of (30), (31) and (32):

$$C_D h \doteq 4\theta_l^* \tag{34}$$

Thus we find that the (normalized) viscous force of the nozzle cusp is equal to the momentum defect of its wake $C_D h$ and also approximately equal to four times the boundary layer momentum thickness at the nozzle trailing edge. Although this section deals with laminar flow on the nozzle cusp, equations (30) and (34) are valid for turbulent flow as well.

As a result of the above, we can now combine (31) and (34) into

$$C_D h = \left(\frac{2 l C_L}{\sqrt{Re_{\infty l}}}\right) Fi \tag{35}$$

In the GDL problem, in which the nozzle axes of symmetry are separated by a distance h_1 according to Fig. 1, it will be convenient to refer all distances

8

to h_1; thus,

$$\frac{C_D h \sqrt{Re_{\infty l}}}{2 l C_L} = \frac{C_D h}{h_1} \frac{h_1}{l} \frac{l \sqrt{Re_{\infty l}}}{2 C_L l} = \left(\frac{C_D h}{h_1}\right) \frac{\sqrt{Re_{\infty h_1}}}{2 C_L} \left(\frac{h_1}{l}\right)^{\frac{1}{2}} = Fi \qquad (36)$$

from which:

$$\frac{C_D h}{h_1} \sqrt{Re_{\infty h_1}} = 2 C_L \sqrt{\frac{l}{h_1}} Fi \equiv \mathcal{F}(M_\infty, \gamma) \qquad (37)$$

with $2C_L = 1.328$. This last equality is possible because, due to geometric similarity, GDL nozzles have a length-to-exit-height ratio dependent on M_∞ (see Ref. 1).

The net result, expressed by (37), then is that the momentum defect of wakes shed from GDL nozzle cusps, expressed as a fraction of the nozzle exit height h_1, is inversely proportional to the square root of the exit Reynolds number

$$Re_{\infty h_1} \equiv \frac{\rho_\infty u_\infty h_1}{\mu_\infty} \qquad (38)$$

and directly proportional to a function $\mathcal{F}$ of the exit Mach number and γ. The function $\mathcal{F}$ has been computed and is shown on Table V. The inverse proportionality to Reynolds number is fully expected for laminar flows. As Table V also shows, $\mathcal{F}$ greatly increases with Mach number and generally decreases with γ. The function $\mathcal{F}$ is also shown on Fig. 3.

6.2 HEAT EXCHANGE IN LAMINAR FLOW

For laminar wakes we take the following expression to represent the energy flux (energy/area/time) from the nozzle surface:

$$q_w = \frac{1}{6^{2/3}} \frac{C_f}{2} \rho u c_p (T_w - T_0) \qquad (39)$$

The total energy exchange per unit span will then be

$$\bar{Q} \equiv 2 \int_0^l q_w \, dz = \frac{\alpha l}{6^{2/3}} \int_0^1 C_f \, \rho u c_p T_0 \, d\left(\frac{z}{l}\right) \qquad (40)$$

9

where

$$\alpha \equiv \frac{T_w}{T_0} - 1 \tag{41}$$

so that if $T_w < T_0$ (cooled plate), $\bar{Q} < 0$ also. Thus $\bar{Q}$ is negative for heat flowing into the nozzle and positive if heat is flowing from the nozzle to the fluid.

From (40) we get, for c_p = constant,

$$\frac{1}{h_1} \frac{\bar{Q}}{\rho_\infty u_\infty c_p T_\infty} = \frac{\alpha \ell}{\sigma^{2/3}} \frac{T_0}{T_\infty} \int_0^1 \frac{\rho u}{\rho_\infty u_\infty} c_f \, d\left(\frac{z}{\ell}\right) =$$

$$= \frac{1}{h_1} \frac{\alpha \ell C_L}{\sigma^{2/3} \sqrt{Re_\infty \ell}} \frac{\beta_\infty^{1.38 + \frac{\gamma+1}{4(\gamma-1)}}}{\sqrt{M_\infty}} \int_0^1 \sqrt{M} \, \beta^{-\frac{\gamma+1}{4(\gamma-1)} - 0.38} \sqrt{\frac{\ell}{z}} \, d\left(\frac{z}{\ell}\right) \tag{42}$$

Physically this parameter is the ratio of the heat exchanged between nozzle cusp and flow, to the heat content of the flow exiting the nozzle. For later purposes, it is necessary to know the corresponding ratio for the kinetic "power" exiting the nozzle:

$$Q \equiv \frac{\bar{Q}}{\frac{1}{2} \rho_\infty u_\infty^3 c_D h} = \left(\frac{\bar{Q}}{\rho_\infty u_\infty c_p T_\infty}\right) \frac{1}{u_\infty^2} \frac{c_p T_\infty}{\frac{1}{2} c_D h} =$$

$$= \left(\frac{\bar{Q}}{\rho_\infty u_\infty c_p T_\infty}\right) \frac{c_p}{\gamma R M_\infty^2} \frac{1}{\frac{1}{2} c_D h} = \left(\frac{\bar{Q}}{\rho_\infty u_\infty c_p T_\infty}\right) \frac{1}{\frac{1}{2} c_D h (\gamma-1) M_\infty^2} \tag{43}$$

If the integral in (42) is called

$$i' \equiv \int_0^1 \sqrt{M} \, \beta^{-\frac{\gamma+1}{4(\gamma-1)} - 0.38} \sqrt{\frac{\ell}{z}} \, d\left(\frac{z}{\ell}\right) = i'(M_\infty, \gamma) \tag{44}$$

(see Table VI for i' values) then

10

$$Q = \frac{\alpha \, \ell \, c_L}{\sigma^{2/3} \sqrt{Re_{\omega \ell}}} \left(\frac{\beta_\infty^{1.38 + \frac{\gamma+1}{4(\gamma-1)}}}{\sqrt{M_\infty}} \right) \frac{2 i'}{c_D h (\gamma-1) M_\infty^2} \tag{45}$$

Using (35), we get

$$\frac{Q}{\alpha} = \frac{1}{\sigma^{2/3}} \frac{\beta_\infty^{1.38 + \frac{\gamma+1}{4(\gamma-1)}}}{(\gamma-1) M_\infty^2} \frac{i'}{i F} \equiv S(M_\infty, \gamma) \tag{46}$$

or

$$Q = \alpha S = \left(\frac{T_w}{T_o} - 1 \right) S(M_\infty, \gamma) \tag{47}$$

The quantity Q, which will feature prominently in the prediction of wake temperature, thus depends on a new entity, the wall-to-stagnation temperature ratio, and the parameter S. The latter can be considered to be the "efficiency" of cooling or heating the wake by cooling or heating the nozzle; it is shown on Table VII and Fig. 4. As with $\bar{Q}$, $Q<0$ if the nozzle is cooled ($T_w<T_o$) and $Q>0$ if the nozzle is heated. Note that $Q = -S$ is the minimum physically attainable, within the present approximations.

The results of Fig. 4 and Table VII indicate that S is highest at low M_∞ and small γ, and lowest at high M_∞ and large γ. This result has also been verified for the simple case of a flat plate at constant flow conditions U_∞, M_∞, etc. Using the Reynolds analogy

$$C_H = \frac{c_f}{2 \sigma} \tag{48}$$

for laminar flow and the relation between the T.E. momentum thickness θ^*_ℓ and $c_D h$ ($\theta^*_\ell = c_D h/4$), it was shown that

$$\frac{Q}{\alpha} = \frac{1}{\sigma} \left[\frac{1}{(\gamma-1) M_\infty^2} + \frac{1}{2} \right] \tag{49}$$

which has the same qualitative behavior with M_∞ and γ as the curves of Fig. 4. This result is physically connected to the definition of Q (see Eq. (42)) which is the proper definition for calculating wake properties (Section 7).

6.3 VISCOUS DRAG IN TURBULENT FLOW

As for the laminar case, the total viscous drag of the nozzle cusp per unit span is given by Eq. (5):

$$\frac{F_v}{\frac{1}{2} \rho_\infty u_\infty^2} = c_D h = 2 \ell \int_0^1 c_f \frac{\rho}{\rho_\infty} \frac{u}{u_\infty^2} \, d\left(\frac{\zeta}{\ell} \right) \tag{50}$$

11

where C_f will now be taken from Ref. 2 to be typical for turbulent flow:

$$c_f = 0.0262 \left(\frac{2}{2 + \frac{\gamma-1}{2}M^2} \right)^{\frac{5}{7}} Re_{\zeta}^{-\frac{1}{7}} = C_T f(M) Re_{\zeta}^{-\frac{1}{7}} \qquad (51)$$

The dependence of c_f on turbulent heat transfer is neglected consistently with assumption D, Section 3. If c_f is then re-written as

$$c_f = \frac{C_T}{(Re_{\infty \ell})^{1/7}} f(M) \left(\frac{\ell}{\zeta} \right)^{1/7} \left(\frac{\rho_\infty u_\infty}{\rho u} \right)^{1/7} \left(\frac{\mu}{\mu_\infty} \right)^{1/7} \qquad (52)$$

we get

$$c_D h = 2\ell \frac{P_0}{P_\infty} \frac{1}{M_\infty^2} \frac{C_T}{Re_{\infty \ell}^{1/7}} \int_0^1 f(M) \left(\frac{\ell}{\zeta} \right)^{1/7} \left(\frac{\rho_\infty u_\infty}{\rho u} \right)^{1/7} \left(\frac{\mu}{\mu_\infty} \right)^{1/7} \frac{P}{P_0} M^2 d\left(\frac{\zeta}{\ell} \right) \qquad (53)$$

This expression can be further reduced to

$$c_D h = 2\ell \frac{P_0}{P_\infty} \frac{1}{M_\infty^2} \frac{C_T}{Re_{\infty \ell}^{1/7}} \left(\frac{A^*}{A} \right)^{1/7} \left(\frac{\gamma+1}{2} \right)^{-\frac{\gamma+1}{14(\gamma-1)}} \left(\frac{\mu_0}{\mu_\infty} \right)^{1/7} i''(M_\infty, \gamma) \qquad (54)$$

where

$$i'' \equiv \int_0^1 \left(\frac{2}{2 + \frac{\gamma-1}{2}M^2} \right)^{5/7} \left(\frac{\ell}{\zeta} \right)^{1/7} M^{-1/7} \beta_\infty^{\frac{\gamma+1}{14(\gamma-1)} - 0.109 - \frac{\gamma}{\gamma-1}} M^2 d\left(\frac{\zeta}{\ell} \right) \qquad (55)$$

This integral has been calculated and is shown on Table VII. The factor of this integral, furthermore, can be also reduced so that (54) finally reads

$$\frac{c_D h (Re_{\infty \ell})^{1/7}}{2 C_T \ell} = M_\infty^{-\frac{13}{7}} \beta_\infty^{0.109 + \frac{\gamma}{\gamma-1} - \frac{\gamma+1}{14(\gamma-1)}} i'' = N i'' \qquad (56)$$

The factor $N(M_\infty, \gamma)$ appears on Table IX.

As was done with the laminar case (eq. (37)), we can express the last result in terms of h_1 as follows:

12

$$\frac{c_D h \left(Re_{\infty h_1}\right)^{\frac{1}{7}}}{h_1} = 2 C_T \left(\frac{\ell}{h_1}\right)^{4/7} Ni'' \equiv G(M_\infty, \gamma) \tag{57}$$

with $2C_T = 2 \times 0.0262 = .05424$. This quantity is tabulated in Table X and also plotted on Fig. 5. It is interesting to compare Fig. 5 with Fig. 3 and, considering Eq. (34), to see how the boundary layer momentum thickness θ^*_ℓ at the T.E. behaves in laminar and turbulent flows. It is seen that $c_D h/h_1$ (and θ^*_ℓ) in both cases increases with M_∞ and decreases with γ. Quantitatively, however, there are differences in magnitude between the two cases because of the Reynolds number exponent (compare Eq. (34) with (56)). For example, if $Re_{\infty h_1} = 10^6$*:

Laminar case: $\quad c_D h / h_1 = 0.0062 \tag{58}$

Turbulent case: $\quad\quad\quad\quad = 0.0123 \tag{59}$

However, in practical circumstances $Re_{\infty h_1}$ is usually much larger if the flow is turbulent; thus for a laminar flow with $Re_{\infty h_1} = 10^5$ the $c_D h/h$ is larger ($=0.0196$) than it is for a turbulent flow with $Re_{\infty h_1} = 10^7$ ($=0.0088$).

6.4 HEAT EXCHANGE IN TURBULENT FLOW

In contrast to the laminar case, the heat transfer coefficient in the turbulent case obeys the Reynolds analogy directly:

$$c_H = \frac{c_f}{2} \tag{60}$$

Thus, with the Prandtl number missing in the heat flux equation (40), the dimensional heat transfer rate from the entire nozzle is

$$\frac{\bar{Q}}{\rho_\infty u_\infty c_p T_\infty} = \alpha \ell \frac{T_0}{T_\infty} \int_0^1 \frac{\rho u}{\rho_\infty u_\infty} c_f \, d\left(\frac{3}{\ell}\right) \tag{61}$$

with α defined again as in (41). Thus,

$$Q \equiv \frac{\bar{Q}}{\frac{1}{2} \rho_\infty u_\infty^3 c_D h} = \frac{2}{(\gamma-1) M_\infty^2 c_D h} \alpha \ell \int_0^1 \frac{\rho u}{\rho_\infty u_\infty} c_f \, d\left(\frac{3}{\ell}\right) \tag{62}$$

Using the turbulent skin friction coefficient from Eq. (51), we obtain

$$\frac{Q}{\alpha} = \frac{Ji'''}{Ni''} = \frac{Q}{\alpha}(M_\infty, \gamma) \tag{63}$$

*These examples are computed for $M_\infty = 4$, $\gamma = 1.4$

where:

$$J \equiv \frac{\beta_\infty}{(\gamma-1)M_\infty^2} \left(\frac{A_\infty}{A^*}\right)^{6/7} \left(\frac{\mu_0}{\mu_\infty}\right)^{1/7} \left(\frac{\gamma+1}{2}\right)^{\frac{3}{7}\frac{\gamma+1}{\gamma-1}} \tag{64}$$

$$\beta_\infty \equiv 1 + \frac{\gamma-1}{2} M_\infty^2 \tag{65}$$

$$i''' \equiv \int_0^1 f(M)\left(\frac{\ell}{\lambda}\right)^{\frac{1}{7}} M^{\frac{6}{7}} \beta^{-\frac{3}{7}\frac{\gamma+1}{\gamma-1} - 0.109} d\left(\frac{\lambda}{\ell}\right) \tag{66}$$

$$f(M) = \left(\frac{2}{2 + \frac{\gamma-1}{2} M^2}\right)^{\frac{5}{7}} \tag{67}$$

N from Table IX

i'' from Eq. (54) and Table VIII.

The quantity Q/α, which is again considered as a heating "efficiency" of the nozzle, appears in Table XI and Fig. 6. As in the laminar flow case (Fig.4), Q/α decreases with increasing M_∞ and also with increasing γ. Comparing Fig. 4 with 6, we also observe that the heat exchange is more efficient in turbulent flow but only at the higher M_∞ and larger γ. In practical terms, however, caution in interpreting this result is needed because of the manner of defining Q (see Eq. (62)).

7. THEORY OF WAKE DECAY

7.1 LAMINAR WAKES

7.1.1 KUBOTA'S LINEARIZED SIMILARITY THEORY FOR COMPRESSIBLE WAKES

Kubota (Ref. 3) has discovered similarity solutions of the boundary layer equations as used to describe two-dimensional, laminar, compressible wakes. For completeness, his results are given here in outline. We will adopt Kubota's notation: subscript 0 (as in ( )$_0$) refers to the wake conditions at some arbitrary initial station; ( )$_e$ refers to conditions just external to and ( )$_\infty$ to conditions very far away from the wake. An overbar, ($^-$) refers to physical (dimensional) coordinates.*

Kubota's coordinates are:

Longitudinal distance:
$$x \equiv \frac{1}{\bar{d}} \int_0^{\bar{x}} \frac{\bar{\rho}_e \bar{\mu}_e \bar{u}_e}{\bar{\rho}_\infty \bar{\mu}_\infty \bar{u}_m} d\bar{x} \tag{68}$$

Lateral distance:
$$y \equiv \frac{\bar{u}_e}{\bar{u}_\infty \bar{d}} \sqrt{Re} \int_0^{\bar{y}} \frac{\bar{\rho}}{\bar{\rho}_\infty} d\bar{y} \tag{69}$$

---

*This subscript notation applies to this Section only. In Section 7.1.2 we return to our own notation.

where $\bar{d}$ is a characteristic (constant) length and

$$Re \equiv \frac{\bar{\rho}_\infty \bar{u}_\infty \bar{d}}{\bar{\mu}_\infty} \tag{70}$$

His solutions are:

$$w \equiv \frac{\bar{u}_e - \bar{u}}{\bar{u}_e} = \frac{A'}{\bar{u}_e^2 \sqrt{x}} e^{-\frac{y^2}{4x}} - \frac{B'}{2\bar{u}_e^2} \int_0^x \frac{d\bar{u}_e^2}{d\zeta} \frac{e^{-\frac{\sigma y^2}{4[\sigma x + (1-\sigma)\zeta]}}}{\sqrt{\sigma x + (1-\sigma)\zeta}} d\zeta \tag{71}$$

$$h \equiv \frac{\bar{T} - \bar{T}_e}{\bar{T}_e} = \frac{B'}{\sqrt{x}} e^{-\sigma y^2/4x} \tag{72}$$

$$\frac{\bar{H}}{H_e} - 1 = \frac{1}{(1 + \frac{\gamma-1}{2} M_e^2)\sqrt{x}} \left(B' e^{-\sigma y^2/4x} - \frac{A'}{h_{eo}} e^{-y^2/4x} \right) \tag{73}$$

$$A' \equiv \bar{u}_{eo}^2 \frac{(\bar{\rho}_e \bar{u}_e \bar{\theta})_o}{\bar{\rho}_\infty \bar{u}_\infty \bar{d}} \sqrt{\frac{Re}{\pi}}, \quad B' \equiv \left[(\gamma-1) M_e^2 \frac{(\bar{\rho}_e \bar{u}_e \bar{\theta})_o}{\bar{\rho}_\infty \bar{u}_\infty \bar{d}} + \frac{\bar{Q}}{2\bar{\rho}_\infty \bar{u}_\infty \bar{d} c_p \bar{T}_{eo}} \right] \sqrt{\frac{\sigma Re}{\pi}} \tag{74}$$

$$\bar{\theta} \equiv \frac{\bar{\rho}_\infty \bar{u}_\infty \bar{d}}{\bar{\rho}_e \bar{u}_e \sqrt{Re}} \int_0^\infty w \, dy \tag{75}$$

The quantities w, h and $\bar{\theta}$ are the fluid velocity and temperature and the momentum thickness, respectively.

7.1.2 ADAPTATION OF KUBOTA'S THEORY TO THE PRESENT PROBLEM

In this section, we will re-write Kubota's formulas (68-75) adapting them to our nomenclature and subjecting them to simplifications suitable to the GDL nozzle problem.

In the present problem we shall assume:

- "The nozzle exhaust flow outside the wake is everywhere uniform."

This assumption approximates well the flow exiting ideal, well-designed nozzles with thin trailing edges in parallel flow. Thus, quantities subscribed by "0" or "e" in eqs. (68-75) become equal to those subscribed by "∞".

15

Still within his nomenclature but under our present conditions, Kubota's equations (67) and (68) then become

$$x \equiv \frac{\bar{x}}{d} \quad , \quad y \equiv \frac{\sqrt{Re}}{d} \int_0^{\bar{y}} \frac{\bar{\rho}}{\bar{\rho}_\infty} \, d\bar{y} \equiv \frac{\sqrt{Re}}{d} \, \tilde{y} \tag{76}$$

where $\tilde{y}$ is the familiar (transformed) compressible coordinate:

$$\tilde{y} = \int_0^{y} \frac{\bar{\rho}}{\bar{\rho}_\infty} \, d\bar{y} \quad , \quad d\tilde{y} = \frac{\bar{\rho}}{\bar{\rho}_\infty} \, d\bar{y} \tag{77}$$

so that, also

$$dy = \frac{\sqrt{Re}}{d} \, \frac{\bar{\rho}}{\bar{\rho}_\infty} \, d\bar{y} \tag{78}$$

Kubota's central approximation ("linearization") consists of assuming, as we will also in this work, that

$$w \ll 1 \tag{79}$$

Then his momentum thickness, from Eq. (74) is

$$\bar{\theta} = \frac{d}{\sqrt{Re}} \int_0^\infty w \, dy \simeq \frac{d}{\sqrt{Re}} \int_0^\infty w \, (1-w) \, \frac{\sqrt{Re}}{d} \, \frac{\rho}{\rho_\infty} \, d\bar{y} -$$

$$= \int_0^\infty w \, (1-w) \, \frac{\bar{\rho}}{\bar{\rho}_\infty} \, d\bar{y} = \cdots = \int_0^\infty \frac{\bar{\rho}\bar{u}}{\bar{\rho}_\infty \bar{u}_\infty} \left(1 - \frac{\bar{u}}{\bar{u}_\infty}\right) d\bar{y} = \frac{c_D h}{4} \tag{80}$$

where, from Ref. 4, $c_D h$ is the "momentum thickness" of the wake:

$$c_D h \equiv 4 \int_0^\infty \frac{\bar{\rho}\bar{u}}{\bar{\rho}_\infty \bar{u}_\infty} \left(1 - \frac{\bar{u}}{\bar{u}_\infty}\right) d\bar{y} \tag{81}$$

We thus see that Kubota's "momentum thickness" $\bar{\theta}$ is actually equal to the momentum thickness θ^*, of the boundary layer on the T.E. of a flat plate generating the wake (see Eq. (34) also).

Another modification to Kubota's theory has to do with x. In our nomenclature, Δx is the distance downstream of the wake "virtual origin", located at x_0.

16

Thus, Kubota's x should be changed to

$$\Delta x = x - x_o \tag{82}$$

Because of previous assumptions, pressure gradients around the wake are neglected:

$$\frac{d}{dx} = \frac{d}{dy} = 0 \tag{83}$$

We are now ready to obtain the flow properties in the wake. <u>Overbars on physical (dimensional) properties are excluded from here on. Also, from here on we return to our own nomenclature (see list of symbols and Fig. 1)</u>.

7.1.2.1 VELOCITY DEFECT FOR LAMINAR FLOW

Using Eq. (82) and (83), in (71) we obtain on the wake axis ($y = \tilde{y} = 0$):

$$w = \frac{u_\infty - u(0)}{u_\infty} = \frac{A'}{u_\infty^2} \frac{1}{\sqrt{\Delta x / d}} \tag{84}$$

$$A' = u_\infty^2 \frac{\theta^*}{d} \sqrt{\frac{Re}{\pi}} = u_\infty^2 \frac{c_D h}{4d} \sqrt{\frac{Re}{\pi}} \tag{85}$$

Thus,

$$w = \frac{c_D h}{4d} \sqrt{\frac{Re}{\pi}} \sqrt{\frac{d}{x}} = \frac{c_D h}{4} \sqrt{\frac{Re'}{\pi}} \frac{1}{\sqrt{\Delta x}} \tag{86}$$

where $Re' \equiv$ unit Reynolds number $= \rho_\infty u_\infty / \mu_\infty$. In the GDL problem it will be convenient to normalize distances with h_1, the nozzle exit height (Fig. 1). Thus,

$$w = \frac{c_D h}{4 h_1 \sqrt{\pi}} \sqrt{Re_{\infty h_1}} \left(\frac{h_1}{\Delta x} \right)^{1/2} \tag{87}$$

and using Eq. (37), we find that

$$w = \frac{1}{4\sqrt{\pi}} \left(\frac{h_1}{\Delta x} \right)^{\frac{1}{2}} \mathcal{F}(M_\infty, \gamma) \tag{88}$$

Thus the velocity defect on the wake centerplane depends only on the downstream distance and on the exit Mach number (and γ). Surprisingly, there is no Reynolds number dependence. If the virtual origin x_o is known, w can thus be found immediately from the $\mathcal{F}$ values of Table V, as computed in Section 6.1.

17

7.1.2.2 TEMPERATURE DEFECT IN LAMINAR FLOW

At $y = \tilde{y} = 0$, Eq. (72) gives, combined with (88):

$$t \equiv \frac{T(0) - T_\infty}{T_\infty} = \frac{B'}{\sqrt{\Delta x}} \tag{89}$$

with

$$B' = \left[(\gamma - 1) M_\infty^2 \frac{c_D h}{4} + \frac{\bar{Q}}{2 \rho_\infty u_\infty c_p T_\infty} \right] \sqrt{\frac{\sigma Re'}{\pi}} \tag{90}$$

Thus,

$$t = \sqrt{\frac{c_D h}{\Delta x}} (\gamma - 1) M_\infty^2 \frac{1}{4} \left[1 + \frac{\bar{Q}}{\frac{1}{2} c_D h \rho_\infty u_\infty c_p T_\infty (\gamma - 1) M_\infty^2} \right] \sqrt{\frac{\sigma}{\pi}} \sqrt{Re_{c_D h}} \tag{91}$$

where

$$Re_{c_D h} \equiv \frac{\rho_\infty u_\infty c_D h}{\mu_\infty} \tag{92}$$

Invoking Eq. (37) and (42), we finally get

$$t = \frac{T(0) - \bar{T}_\infty}{T_\infty} = \sqrt{\sigma} \, (\gamma - 1) M_\infty^2 (1 + Q) W \tag{93}$$

Thus the temperature on the wake centerplane is seen to depend on the laminar Prandtl number σ, ratio of specific heats γ, exit Mach number M_∞ and the non-dimensional heat exchange rate Q, defined in Eq. (42) and tabulated in Table VII (see also Fig. 4). Note that, from Eq. (47),

$$Q < 0 \quad \text{IF} \quad T_w / T_o < 1 \tag{94}$$

Thus, t decreases if the nozzle surface temperature decteases below T_o.

7.1.2.3 PRESSURE DEFECT IN LAMINAR FLOW

Consistent with Kubota's assumptions, the pressure everywhere inside the wake is assumed to be constant and equal to the GDL nozzle exit pressure p_∞.

7.1.2.4 DENSITY DEFECT IN LAMINAR FLOW

Because of the constant-pressure assumption, the density defect can be computed directly from the temperature defect of Eq. (93):

$$r \equiv \frac{\rho_\infty - \rho(0)}{\rho_\infty} = \frac{t}{t + 1} \tag{95}$$

18

Thus, the density defect does not show the $(\Delta x/h_1)^{-\frac{1}{2}}$ decay behavior exhibited by the velocity and temperature defects.

7.1.2.5 TOTAL TEMPERATURE DEFECT IN LAMINAR FLOW

From Kubota's Eq. (73), using our nomenclature, we obtain at $y = \tilde{y} = 0$:

$$\Theta \equiv \frac{T_0(0) - T_{0\infty}}{T_{0\infty}} = \frac{\sqrt{d}}{\beta_\infty \sqrt{\Delta x}} \left(B' - \frac{A'}{c_p T_\infty} \right) \tag{96}$$

where, again

$$\beta_0 = 1 + (\gamma - 1) M_\infty^2 / 2 \tag{97}$$

Inserting the expression for Q (Eq. (42)) into B' (Eq. (73)), we get

$$B' = \frac{c_D h}{4} (\gamma - 1) M_\infty^2 \frac{1}{d} \sqrt{\frac{\sigma Re}{\pi}} \left[1 + \frac{\bar{Q}}{\frac{1}{2} c_D h (\gamma - 1) M_\infty^2 \rho_\infty c_p u_\infty T_\infty} \right] =$$

$$= \frac{c_D h}{4} (\gamma - 1) M_\infty^2 \frac{1}{d} \sqrt{\frac{\sigma Re}{\pi}} (1 + Q) \tag{98}$$

Also, from Eq. (73) for A':

$$\frac{A'}{c_p T_\infty} = (\gamma - 1) M_\infty^2 \frac{c_D h}{4d} \sqrt{\frac{Re}{\pi}} \tag{99}$$

Since $Re \equiv \rho_\infty u_\infty d / \mu_\infty$, and using Eq. (88) for w,

$$\Theta = \frac{1}{\beta_\infty} \sqrt{\frac{d}{\Delta x}} \frac{c_D h}{4} \frac{1}{d} (\gamma - 1) M_\infty^2 \sqrt{\frac{Re}{\pi}} \left[\sqrt{\sigma} (1 + Q) - 1 \right] \tag{100}$$

or

$$\Theta \equiv \frac{T_0(0) - T_{0\infty}}{T_{0\infty}} = \frac{(\gamma - 1) M_\infty^2 w}{\beta_\infty} \left[\sqrt{\sigma} (1 + Q) - 1 \right] \tag{101}$$

where w is again given by (88).

19

7.1.2.6 LATERAL LAMINAR VELOCITY VARIATION, AND THE TRANSVERSE SCALE

From Kubota's Eq. (71) we get, in our nomenclature

$$\tilde{u} \equiv \frac{u_\infty - u}{u_\infty - u(0)} = \frac{w}{w(y=0)} = e^{-y^2/4x} = \exp\left[-\frac{Re}{f}\frac{\tilde{y}^2}{d^2}\frac{d}{\Delta x}\right] \tag{102}$$

Inserting (86) into (102) we get:

$$\tilde{u} = \exp\left[-\tilde{y}^2\frac{\pi}{4}\left(\frac{16w^2}{(c_D h)^2}\right)\right] \tag{103}$$

Define a <u>transverse scale</u> L and a dimensionless lateral coordinate η by

$$L \equiv \frac{c_D h}{4w} \quad , \quad \eta \equiv \frac{\tilde{y}}{L} = \frac{1}{L}\int_0^y \frac{\rho}{\rho_\infty}\,dy \tag{104}$$

Thus,

$$\tilde{u} = e^{-\frac{\pi}{4}\eta^2} = e^{-0.785\eta^2} \tag{105}$$

Note that since $c_D h$ is a function of the Reynolds number according to Eq. (37) and Fig. 3, the lateral velocity variation is also a function of the Reynolds number.

7.1.2.7 LATERAL TEMPERATURE VARIATION IN LAMINAR FLOW

From Eq. (72) we arrive at the counterpart of Eq. (105) for the temperature:

$$\tilde{T} \equiv \frac{T - T_\infty}{T(0) - T_\infty} = e^{-\frac{\pi\sigma}{4}\eta^2} = e^{-0.785\sigma\eta^2} \tag{106}$$

7.1.2.8 LATERAL PRESSURE VARIATION IN LAMINAR FLOW

The static pressure p_∞ is constant across and along the wake.

20

7.1.2.9   LATERAL DENSITY VARIATION IN LAMINAR FLOW

Because of the constancy of pressure, the lateral density variation is given by

$$\tilde{\rho} \equiv \frac{\rho_\infty - \rho}{\rho_\infty - \rho(0)} = \frac{\tilde{T}(t+1)}{\tilde{T}t + 1} \tag{107}$$

with $\tilde{T}$ and t supplied by Eq. (106) and (93), respectively. Thus, as is well known (Ref. 4) the lateral density profile is not similar (i.e., $\tilde{\rho}$ depends on Δx through t) until $t = 0$, which of course occurs only asymptotically, far downstream.

7.1.2.10   LATERAL TOTAL TEMPERATURE VARIATION IN LAMINAR FLOW

From the formulas presented so far, we can show that since

$$\tilde{T}_0 \equiv \frac{T_0 - T_{0\infty}}{T_0(0) - T_{0\infty}} = \frac{T/T_{0\infty} - 1}{T_0(0)/T_{0\infty} - 1} = \frac{B' e^{-\sigma y^2/4x} - (A'/c_p T_\infty) e^{-y^2/4x}}{B' - A'/c_p T_\infty} \tag{108}$$

then

$$\tilde{T}_0 = \frac{\sqrt{\sigma}(1+Q)e^{-\frac{\sigma\pi}{4}\eta^2} - e^{-\frac{\pi}{4}\eta^2}}{\sqrt{\sigma}(1+Q) - 1} = T_0(\eta; \sigma, Q) \tag{109}$$

which is a similarity solution.

Fig. 7 shows the lateral profiles of velocity, temperature, density and total temperature in the laminar-wake case, the last three for $\sigma = 0.75$.

7.1.2.11   APPROXIMATE CALCULATION OF LAMINAR WAKE THICKNESS

We define the "transformed velocity half thickness" as the lateral distance $\tilde{y}u$ at which $\tilde{u}$, from Eq. (105), has decreased to a certain level. The choice of this level is arbitrary, and will be taken here as 0.01:

$$\tilde{u}_u = 0.01 \tag{110}$$

Then from Eq. (105) it can be shown that

$$\frac{\tilde{y}_u}{h_1} = 4.29 \sqrt{\frac{\Delta x/h_1}{Re_{\infty h_1}}} \tag{111}$$

where

$$Re_{h_1} \equiv \rho_\infty u_\infty h_1 / \mu_\infty \tag{112}$$

21

Because of symmetry about the wake centerplane (axis), then the (full) velocity thickness is

$$\frac{\widetilde{b_u}}{h_1} \equiv 2 \frac{\widetilde{y_u}}{h_1} = 8.58 \sqrt{\frac{\Delta x / h_1}{Re_{\infty h_1}}} \tag{113}$$

with analogous results for the transformed temperature thickness:

$$\frac{\widetilde{b_T}}{h_1} = \frac{8.58}{\sqrt{\sigma}} \sqrt{\frac{\Delta x / h_1}{Re_{\infty h_1}}} \tag{114}$$

It will be desirable to have a formula for the physical thicknesses. This is impossible to do in the context of similarity because the density ratio depends on x (see Eq. (107)).

A serviceable approximation can be had by assuming that this ratio varies linearly with y:

$$\frac{\rho(y)}{\rho_\infty} \simeq \frac{y}{y_t} \left(1 - \frac{\rho(0)}{\rho_\infty} \right) y + \frac{\rho(0)}{\rho_\infty} \tag{115}$$

where y_t is the physical wake "edge." Then,

$$\widetilde{y_t} \equiv \int_0^{y_t} \frac{\rho}{\rho_\infty} \, dy = \int_0^{y_t} \left[\frac{y}{y_t} \left(1 - \frac{\rho(0)}{\rho_\infty} \right) y + \frac{\rho(0)}{\rho_\infty} \right] dy \simeq$$

$$\simeq \frac{y_t}{2} \left[1 + \frac{\rho(0)}{\rho_\infty} (x) \right] \tag{116}$$

or

$$y_t = \frac{2 \widetilde{y_t}}{1 + \frac{\rho(0)}{\rho_\infty}} \tag{117}$$

and since, from (107)

$$1 + \frac{\rho(0)}{\rho_\infty} = \frac{t+2}{t+1} \tag{118}$$

we get for the plysical thicknesses,

$$b_u / h_1 = \frac{17.16 (t+1)}{t+2} \sqrt{\frac{\Delta x / h_1}{Re_{\infty h_1}}} \tag{119}$$

22

$$\frac{b_T}{h_1} = \frac{1}{\sqrt{6}} \frac{b_u}{h_1} \qquad (120)$$

These quantities are the only ones calculated so far for the laminar wake, which depend on the Reynolds number.

7.2 TURBULENT WAKES

7.2.1 LINEARIZED SIMILARITY THEORY FOR TURBULENT WAKES

Since no straightforward turbulence theory is possible, there exists no formal counterpart of Kubota's theory which can be developed from first principles when the wake is turbulent. There exists, however, a linearized similarity solution for turbulent flows for the "far wake" limit of $w \ll 1$ (Ref. 4). *This solution involves a single assumption which, as can be expected, indirectly concerns the turbulent viscosity.* The solution, which is supported strongly by experiments (Refs. 4,5, and 6), is very appropriate to use here because of its kinship to the Kubota theory (through the $w \ll 1$ approximation) and because it yields formulas almost exactly the same as presented in *Section 7.1.*

The starting point of the "theory" is the same as for Kubota's theory, e.g., steady, uniform isobaric flow, etc. Then, the key assumption regarding the <u>velocity</u> <u>defect</u> is made:

$$w = \sqrt{\frac{R_T}{10}} \sqrt{\frac{c_D h}{\Delta x}} \qquad (121)$$

where R_T *is the so-called turbulent Reynolds number.*

Assumption (121) now leads to the following results:

7.2.1.1 VELOCITY DEFECT IN TURBULENT FLOW

The velocity defect as given by (121) can be further expressed in the desired coordinates by utilizing Eq. (57):

$$\frac{\Delta x}{c_D h} = \left(\frac{\Delta x}{h_1} \right) \left(\frac{h_1}{c_D h} \right) = \left(\frac{\Delta x}{h_1} \right) \frac{1}{2 c_T i'' N} \left(\frac{h_1}{l} \right)^{6/7} \left(Re_{\infty h_1} \right)^{1/7} \qquad (122)$$

Thus,

$$w = \left(2 c_T \frac{R_T}{10} \right)^{1/2} \left(\frac{h_1}{\Delta x} \right)^{1/2} \left[\frac{i''^{\frac{1}{2}} N^{\frac{1}{2}}}{(Re_{\infty h_1})^{1/14}} \left(\frac{l}{h_1} \right)^{3/7} \right] \qquad (123)$$

23

If we adopt the experimentally known value for R_T from Ref. 4:

$$R_T = 13 \qquad (124)$$

and noting that $C_T = 0.0262$, we obtain

$$W = 0.261 \left(\frac{h_1}{\Delta x} \right)^{1/2} K(M_\infty, \gamma, Re_{\infty h_1}) \qquad (125)$$

where

$$K \equiv \frac{i'' \frac{1}{2} N^{\frac{1}{2}}}{(Re_{\infty h_1})^{1/14}} \left(\frac{\ell}{h_1} \right)^{3/7} \qquad (126)$$

The quantity K has been tabulated in Table XIII for $Re_{\infty h_1} = 10^5$. Note that for other values of $Re_{\infty h_1}$ the K will not change much, since it depends on the former to the 1/14th power, according to Eq. (126).

7.2.1.2 TEMPERATURE DEFECT IN TURBULENT FLOW

$$t \equiv \frac{T(0) - T_\infty}{T_\infty} = \sqrt{\sigma}_T \, (\gamma - 1) M_\infty^2 \, (1 + Q) W \qquad (127)$$

where Q is defined exactly as before (Eq. (42)).

7.2.1.3 DENSITY AND PRESSURE DEFECTS IN TURBULENT FLOW

As for the laminar flow, the pressure is everywhere constant, and

$$r \equiv \frac{\rho_\infty - \rho(0)}{\rho_\infty} = \frac{t}{t + 1} \qquad (128)$$

7.2.1.4 TOTAL TEMPERATURE DEFECT IN TURBULENT FLOW

$$\Theta = \frac{(\gamma - 1) M_\infty^2 W}{\beta_\infty} \left[\sqrt{\sigma}_T \, (1 + Q) - 1 \right] \qquad (129)$$

7.2.1.5 LATERAL TURBULENT VELOCITY VARIATION

From Ref. 4 we get

$$\tilde{u} = e^{-0.69 \eta^2} \qquad (130)$$

7.2.1.6 LATERAL TURBULENT TEMPERATURE VARIATION

From Ref. 4 we also get

$$\tilde{T} = e^{-0.45 \eta^2} \tag{131}$$

7.2.1.7 LATERAL DENSITY AND PRESSURE VARIATIONS

Again, the pressure is everywhere constant. The lateral density variation $\tilde{\rho}$ is derived exactly as for the laminar wake:

$$\tilde{\rho} \equiv \frac{\rho_\infty - \rho}{\rho_\infty - \rho(0)} = \frac{\tilde{T}(t+1)}{\tilde{T}t + 1} \tag{132}$$

7.2.1.8 LATERAL TURBULENT TOTAL TEMPERATURE VARIATION

The lateral variation of the total temperature is again given by

$$\tilde{T}_0 = \frac{\sqrt{\sigma_T}(1+\alpha)\tilde{T} - \tilde{u}}{\sqrt{\sigma_T}(1+\alpha) - 1} = \frac{T_0 - T_{0\infty}}{T_0(0) - T_{0\infty}} \tag{133}$$

where the $\tilde{T}$ and $\tilde{u}$ are the turbulent lateral variations (Eqs. (130) and (131)).

A note of caution is needed in regard to Eq. (133) (the same applies to the laminar later variation, Eq. (109)).

It can be seen that for

$$Q = \frac{1}{\sqrt{\sigma_T}} - 1 \tag{134}$$

The denominator is zero; since σ is usually of order 0.7 (in laminar or turbulent flow), this condition occurs at $Q \simeq 0.2$, i.e., when the wake (or nozzle) is slightly heated. Physically, the explanation is simple: when heating is applied the wake axis, which is normally at $T(0) < T_{0\infty}$ (as can be verified from (129) when $Q = 0$), begins rising in temperature until $T_0(0) = T_\infty$ or $T_0(0) - T_\infty = 0$.

7.2.1.9 APPROXIMATE CALCULATION OF THE TURBULENT WAKE THICKNESS

From the experimental results of Ref. 4, we note that the transformed "half-thickness" of the turbulent wake (defined as the point where $\tilde{u} = 0.01$) is

$$\tilde{y}_u = 2.58 \, \frac{c_D h}{4w} \tag{135}$$

25

Utilizing the approximate inverse transformation (117) between $\tilde{y}_u$ and y_u, and again calling the "full thickness" $b_u = 2y_u$, we get

$$b_u = 2.58 \frac{t+1}{t+2} \frac{c_D h}{w} \tag{136}$$

Then, utilizing the relation (125) for w in turbulent nozzle flow, we get

$$\frac{b_u}{h_1} = 0.135 \frac{t+1}{t+2} \frac{K^2}{w} = 0.517 \frac{t+1}{t+2} K \left(\frac{\Delta x}{h_1} \right)^{1/2} \tag{137}$$

The quantity K is tabulated in Table XIII for $Re_{\infty h_1} = 10^5$. Note that for other values of $Re_{\infty h_1}$ the K will not change much since it depends on the former to the 1/14th power, according to Eq. (126).

7.3 THE VIRTUAL ORIGIN ASSUMPTION

The formulas presented so far express the variables in terms of the longitudinal coordinate $\Delta x = x - x_0$, where x_0 is the "virtual origin" of the wake. The location of the virtual origin cannot be found from first principles, and must be obtained from experiment. In the meantime, an "educated guess" of x_0 is in order to that some numerical applications of the previous results can be obtained.

Since the wake thickness is finite at the cusp T.E., it is certainly incorrect to locate x_0 there, i.e., to put $x_0 = 0$ (see Fig. 1 for the coordinate convention). Since the nozzle has been assumed to be a flat plate for convenience, and since its wetted length (for friction and heat transfer calculation purposes, see Section 6) has been assumed equal to ℓ, we shall assume that

$$x_0 = -\ell \tag{138}$$

so that the virtual origin for both the laminar and the turbulent wake is assumed to lie at the location of the nozzle throat.

The above assumption means that as it appears in the various formulas, the coordinate

$$\frac{\Delta x}{h_1} \equiv \frac{x}{h_1} - \frac{x_0}{h_1} = \frac{x}{h_1} - \left(-\frac{\ell}{h_1} \right) = \frac{x}{h_1} + \frac{\ell}{h_1} \tag{139}$$

so that, for example, a point lying one unit of h_1 ($x = h_1$) downstream of the T.E. actually lies $1 + \ell/h_1$ downstream of the origin. Since ℓ/h_1 is also

26

a function of M∞, the trailing edge itself ($x = 0$, $\Delta x/h_1 = \ell/h_1$) lies downstream of the origin by an amount dependent on M_∞ given on Table XIV.

7.4 THE TRAILING EDGE NON-EQUILIBRIUM WAKE REGION

It is clear from the above discussion of the virtual origin that, according to the formulas given, the wake will have already diffused at the T.E. position; for example, for laminar flow $M_\infty = 2$, $\gamma = 1.6$, w at the trailing edge is 0.37. Simple physical arguments, however, dictate that at the trailing edge $w = 1$. There will be a region, therefore, in which the wake adjusts from $w = 1$ at the T.E. to the values given by the present theory, and beyond which w follows the $\Delta x/h_1$ dependence given herein. This region is called the "trailing edge (T.E.) non-equilibrium region."*

The extent of the non-equilibrium region can be calculated with difficulty for laminar flows; in turbulent flow the usual hardships about turbulent viscosity are added. In either case, its extent is of course, dependent on the size and shape of the cusp T.E. No such calculations have been attempted herein; however, since the extent of the region should scale with the trailing edge height, the assumption of "sharp" trailing edge adopted here should help keep the non-equilibrium region short.

It should also be stressed that problems arising because of the non-equilibrium region are quite distinct from the problem of meeting the "linearization" criterion $w \ll 1$. That is, even after the flow "loses memory" of the T.E., the w may not be low enough to satisfy the validity criteria of the theory by which it was computed.

---

*In the extensive wake literature, it is also called the "near wake region."

8. APPLICATIONS OF THE THEORIES FOR LAMINAR OR TURBULENT WAKES

8.1 PROCEDURES FOR COMPUTING THE WAKE CHARACTERISTICS

To compute wake decay for GDL nozzle cusps, a set of inputs is necessary:

o Ratio of specific heat γ (140)

o Exit Mach number M_∞ (141)

o Exit Reynolds number Re'_∞ ($\equiv \rho_\infty u_\infty / \mu_\infty$) (142)

o Stagnation (supply) temperature T_0 (143)

o Nozzle wall temperature (average) T_w (144)

o Nozzle exit height h_1 (145)

Note that Re'_∞ can be calculated for any gas if T_0, M_∞ and the supply pressure P_0 are known instead. Note, also, that γ, M_∞ and h_1 alone are sufficient to compute the velocity defect w, since the latter does not depend* on Re'_∞, T_w or T_0.

The first thing to do after the parameters (139)-(144) are known is to determine whether the wake is laminar or turbulent, since the results will be markedly different for these two types of wakes. Wake transition correlations are available for 2-dimensional supersonic wakes, in Refs. 7, 8 and elsewhere. The present formulas are designed to handle "wholly laminar" wakes (laminar boundary layer on the nozzle followed by laminar wake) or "wholly turbulent" wakes (turbulent nozzle boundary layer followed by turbulent wakes.) As already hinted earlier, the transitional case is complex and will be addressed in a later report.

Once the state of the wake is thus determined, the equations of Section 7.1 (together with the appropriate tables) must be used for the laminar case, and those of Section 7.2 for the turbulent case. If laminar wakes are involved, it is necessary to first compute the function $\mathcal{F}$ (Table V) for the given values of M_∞ and γ. This Table already tabulates $\mathcal{F}$ for M_∞ = 2,3,4,5 and 6 and for γ = 1.2, 1.3 . . . . 1.6, 1.667. (Linear interpolation is adequate for intermediate values of M_∞ and γ.) With $\mathcal{F}$ thus known, w can be computed as a function of ($\Delta x/h_1$) from Eq. (88); note the definition of Δx and h_1 from Eq. (139) and Fig. 1. The value of w so found can now be used into Eq. (93) to give $t(\Delta x/h_1)$. In this case, the laminar flow Prandtl

---

*In the laminar case, the Re'_∞ dependence of C_{Dh} cancels the Re'_∞ dependence of w. In the turbulent case w depends so weakly on Re'_∞ (see Eq. (124)) that computation at a typical Re'_∞ will suffice, within a small percentage error, for a wide range of Re'_∞.

number σ is needed (typically $\sigma \simeq 0.7$) and Q can be found from the Q/α of Table VII as follows:

$$Q = \frac{Q}{\alpha} \alpha = \frac{Q}{\alpha} \left(\frac{T_w}{T_D} - 1 \right) \tag{146}$$

where Tw and To are assumed given, as stated above. With M_∞, γ, w, t and Q available, the density and total temperature defects r and Θ (Eqs. (95) and (96) can also be computed. Note that the pressure within and around the wake is constant (and equal to the nozzle exit pressure) everywhere in this formulation.

Since t has been computed from (93), the wake thickness can now be found from (119). In this computation, the nozzle exit Reynolds number Re_{h_1} is also utilized.

The computation of the lateral distributions is somewhat more involved. Having computed w, we next need C_{Dh} for computing L from Eq. (104). By Eq. (37),

$$c_D h = \frac{h_1 \mathcal{F}}{\sqrt{Re_{\infty h_1}}} \tag{138}$$

With L thus known from (104), we can compute η, from Eq. (104), for any (transformed) distance $\mathbf{y}$ off the wake axis; then the velocity at η is computed from (105). The same procedure is followed for the lateral distributions of temperature (from (106)), density (from (107)) and total temperature (from (109)).

If the wake is turbulent the new pertinent function (instead of $\mathcal{F}$), is K, given in Table XIII. Then the required properties are obtained from the formulas of Section 7.2.

8.2 A NUMERICAL EXAMPLE

To illustrate the use of the formulas, we shall compute the following example. A set of GDL nozzles, of exit height 1 cm and kept at temperature 500°K, discharges helium gas at exit Mach number 3. If the supply chamber upstream of the nozzles is kept at a pressure of 100 psia and temperature of 1000°K, let us compute the gas velocity, pressure, temperature, etc., at a point on the wake axis of symmetry lying at 4 cm. downstream of the nozzle cusp trailing edge (for laminar as well as turbulent flow.)

Solution

The quantities given are:

$$M_\infty = 3 \tag{147}$$
$$\gamma = 1.667 \tag{148}$$

29

$$P_O = 100 \text{ psia} \tag{149}$$
$$T_O = 1000^\circ K \tag{150}$$
$$T_W = 500^\circ K \tag{151}$$
$$h_1 = 1 \text{ cm} \tag{152}$$
$$x = 4 \text{ cm} \tag{153}$$

We can first compute the nozzle exit Reynolds number Re_{h_1} from standard references, such as Ref. 9, from the given quantities (147), (148), (149) and (150):

$$Re_{h_1} = 127,000 \tag{154}$$

Also, it is convenient to compute at the outset, the quantity $\Delta x/h_1$ from Eq. (139) the quantity (147) and Table XIV:

$$\frac{\Delta x}{h_1} = \frac{4}{1} + 2.05 = 6.05 \tag{155}$$

We can now solve the problem first by assuming a laminar wake (which is in anyway appropriate since Re_{h_1} is small). From Eq. (88), and using Table V, for the inputs (147) and (148), we get for the velocity defect,

$$W = \frac{1}{4\sqrt{\pi}} (6.05)^{-\frac{1}{2}} (4.456) = 0.255 \tag{156}$$

To compute the temperature defect from (93) we first compute Q as follows: inputing (150) and (151) into Eq. (41):

$$\alpha = -0.5 \tag{157}$$

while for (147) and (148) Table VII gives

$$\frac{Q}{\alpha} = 0.4611, \quad Q = -0.23 \tag{158}$$

Inserting $\sigma = 0.75$ (the typical laminar Prandtl number) as well as (148), (147), (156) and (158) into Eq. (93) we get

$$t = 1.02 \tag{159}$$

The density defect then follows directly from (95):

$$r = 0.505 \tag{160}$$

The total temperature defect Θ can also be found from (101)

$$\Theta = -0.128 \tag{161}$$

30

To compute the wake thickness we utilize (159), (155), (152) and (154) into Eq. (119):

$$b_u = 0.0793 \text{ cm} \tag{162}$$

The physical (dimensional) quantities of interest can now also be computed directly from the last few formulas given above, utilizing the definitions (84), (93), *etc.* For example, for the velocity $u(0)$ and temperature $T(0)$ on the wake axis:

$$u(0) = u_\infty(1-w) \tag{163}$$

$$T(0) = T_\infty(1+t) \tag{164}$$

The stream quantities u_∞ and T_∞ are first evaluated for isentropic flow (using the given quantities) and Ref. 9.

$$u_\infty = 2.79 \times 10^5 \text{ cm/sec} \tag{165}$$

$$T_\infty = 250^\circ K \tag{166}$$

Then,

$$u(0) = 2.08 \times 10^5 \text{ cm/sec} \tag{167}$$

$$T(0) = 505^\circ K \tag{168}$$

For the turbulent wake, the velocity defect is obtained from inserting the value of K from Table XIII, and input (155), into Eq. (125):

$$w = 0.0563 \tag{169}$$

where the present value of Re_{h_l} (input (154)) and that used in setting up Table XIII ($Re_{h_l} = 10^5$) are close enough to make practically no difference.

For the temperature defect, use is made of the same α as before (see (157) and Q/γ from Table XI:

$$Q = 0.5 (0.714) = -0.357 \tag{170}$$

Thus t is, using $\sigma T = 0.7$, from Eq. (127):

$$t = \sqrt{0.7}\left(\frac{2}{3}\right)9 \, (0.643)(0.0563) = 0.182 \tag{171}$$

Then r from Eq. (127) is

$$r = \frac{0.182}{1+0.182} = 0.154 \tag{172}$$

while Θ from Eq. (129) is

$$\Theta = -0.039 \tag{173}$$

31

For the turbulent wake thickness we utilize (171), (152), (155) and the value of K from Table (XIII) into Eq. (137):

$$b_u = 0.517 \frac{1.182}{2.182} (6.05)^{\frac{1}{2}} (0.531) = 0.366 \text{ cm.} \quad (174)$$

Dimensional examples of variables are:

$$u(0) = 2.64 \times 10^5 \text{ cm/sec} \quad\quad\quad (175)$$
$$T(0) = 295^\circ K \quad\quad\quad (176)$$

The results for the laminar and turbulent wake can then be summarized as follows:

Quantity	Laminar	Turbulent
Velocity defect $w = \dfrac{u_\infty - u(0)}{u_\infty}$	0.255	0.0563
Velocity $u(0)$ (cm/sec)	2.08×10^5	2.64×10^5
Temperature defect $t = (T(0) - T_\infty)/T_\infty$	1.02	0.182
Temperature $T(0)$ $^\circ K$	505	296
Density defect $r \equiv (\rho_\infty - \rho(0))/\rho_\infty$	0.505	0.154
Total temperature defect $\ominus \equiv (T_o(0) - T_{o\infty})/T_{o\infty}$	-0.128	-0.039
Thickness (cm)	0.0793	0.366

By their definition the "defects" shown (of velocity, temperature, etc.) are measures of non-uniformities in the GDL cavity; physically they resemble "troughs" cutting through the cavity. We see that the laminar case is distinguished by large defects and thin wakes; the inverse is true for the turbulent case. Thus when the wakes are laminar the troughs are narrow and deep, while in the turbulent case they are broad and shallow.

8.3 NUMERICAL CALCULATIONS FOR $M_\infty = 4$, $\gamma = 1.4$

Detailed numerical computations for the laminar and turbulent cases have been done for the case $M_\infty = 4$, $\gamma = 1.4$ and $Re_{h_1} = 10^5$, using standard values for the Prandtl number ($\sigma = 0.75$, $\sigma_T = 0.7$). These parameters were chosen to correspond to those of current experiments in the Aeronutronic Ford Supersonic Wind Tunnel.

The results of this calculation are shown on Figs. 8 through 12. Fig. 8 shows the velocity defect w for the laminar and turbulent case; this quantity is independent of Tw for both cases. There is no Reynolds number dependence

32

in the laminar case, while in the turbulent case the Re_{h_1}-dependence is extremely weak. Note the large difference (by a factor of 5) between the two cases. In the turbulent case, too, at a downstream distance of 10 nozzle exit heights from the virtual origin (7.5 from the T.E.) the velocity on the wake axis differs from the stream velocity by only a few percent.

The temperature defect t is shown on Fig. 9. Like w, t decays like the inverse square root of distance (obscured in the Figure because of the semi-log plot). Like w, t is only weakly dependent on Re_{h_1} (and then only in the turbulent case.) Note that, as expected, cooling the nozzles also cools the wake in almost an exact proportion to the nozzle temperature drop. In absolute magnitude, however, the wake cools down less: for example, when the nozzle temperature is lowered $360^{O}R$ below a supply temperature of $600^{O}R$, the turbulent wake axis temperature at $\Delta x/h_1 = 10$ is lowered by only $30^{O}R$.

Fig. 10 shows the density defect. As can be seen from Eqs. (95) and (128) the density does not obey the inverse-square-root decay law with ($\Delta x/h_1$). Also, because of the functional form of the Eqs. (127) and (128), the dependence of r on Re_{h_1} is now practically nil in the turbulent case.

It should be stressed, in regard to Figs. 8 through 10, that the various "defects" plotted are, as defined, measures of the flow non-uniformity in the cavity (and, as such, useful concepts for GDL problems). Thus, their general decrease as Tw decreases below To does not mean that the temperature (or density) decreases, but rather that the non-uniformities in the GDL cavity decrease as the nozzle temperature decreases in relation to the supply temperature. Physically this happens because, while the main gas flow is cooled by the expansion process, the wake fluid retains the frictional heat acquired on the nozzle surfaces and tends to be much hotter than the surrounding fluid. This can then be offset by keeping the nozzles cooler relative to the supply chamber.*

One type of defect which increases as Tw is lowered is that of the total temperature, plotted on Fig. 11. We know from Eq. (129) that Θ would be identically zero for unity Prandtl number when Tw = To. The departure of σ (and σ_T) from unity creates a finite Θ, as shown, even for Tw = To. As the temperature Tw is lowered Θ increases negatively, consistent with energy considerations.

Wake thicknesses, as defined in the previous formulas (see Eq. (137) for example) are plotted on Fig. 12. Note that the turbulent wake, irrespective
*From the definition of t and r (e.g. Eq. (127) and (128) it is clear that t can attain, in the limit, a minimum value of -1. When near this limit, t can cause r to be very large and negative in sign, implying $\rho(0) \gg \rho_\infty$. This is physically realistic and implies a very dense wake in this case.

of Reynolds number, is about 6 times thicker than the laminar wake computed for $Re_{h_1} = 10^5$, which is quite possibly at the lowest end of the GDL range-of-interest. The laminar wake depends on the inverse square root of Re_{h_1}, so that any increase in Re_{h_1} will tend to "thin down" the laminar wake. In either laminar or turbulent case it should be kept in mind that b_u/h_1 does not grow as the square root of $(\Delta x/h_1)$, because of the inverse transformation (see Section 7.1.2.11).

By a distance equal to $10(\Delta x/h_1)$ it is seen by Fig. 12 that the laminar wake occupies about 10% of the width of the GDL cavity $(b_u/h_1 \simeq 0.1)$, but the turbulent wake occupies about 60% of the cavity. It is clear, therefore, that the turbulent wake could, in some instances, totally "fill" the GDL cavity.

9. CONCLUSIONS

The device of a "universal family" of DeLaval nozzles has enabled us to connect the integral nozzle properties with the wake properties. Linearized similarity formulas were then derived by which the important wake quantities can be found if the GDL "design" parameters are known. Linearization implies, in practical terms, that the solutions are valid only when w is small, that is not too near the trailing edge. This is so even if the T.E. is ideally "sharp." If the T.E. is truncated, an additional reason will exist for invalidating these solutions immediately downstream of it.

The most remarkable result obtained is that the solutions for most of the laminar wake properties are Reynolds-number-independent. This "Reynolds number independence principle" seems to have been first discovered by Dewey (Ref. 10) for laminar shear layers in separated flow regions. In the present case it arises because the Re-dependence of the nozzle flow cancels the Re-dependence of the wake flow. For the turbulent case there is a corresponding Reynolds-number independence, in the sense that once a computation is done for a typical Re_{h_1} the results are valid for other Re_{h_1} within a broad range, to good accuracy.

If the wake defects are viewed as undesirable inhomogeneities, then one is better off to design for low M_∞ and large γ, and to lower Tw considerably below To. The Reynolds number, according to the present results, is of concern only when the wake is laminar, and even then it affects only the wake thickness.

Finally, it must be stressed that when the wake is turbulent, there are fluctuations superposed on the mean flow field as calculated herein. These fluctuations may be very important from the standpoint of optics, and will be treated in a future report.

REFERENCES

1. Shames, H. and Seashore, F.L.: <u>Design Data for Graphical Construction of Two-Dimensional Sharp-Edge-Throat Supersonic Nozzles</u>, NACA RM E8J12, Washington, D.C. December 1948

2. Shapiro, A.H., <u>The Dynamics and Thermodynamics of Compressible Fluid Flow</u>, Ronald Press, New York, N.Y., 1954, Vol. II, Part VIII

3. Kubota, T., <u>Laminar Wakes with Streamwise Pressure Gradient</u>, GALCIT Hypersonic Research Project IM No. 9, California Institute of Technology, Pasadena, California, May 1962

4. Demetriades, A., <u>Turbulent Mean-Flow Measurements in a Two-Dimensional Supersonic Wake</u>, Physics of Fluids, Vol. 12, No. 1, p 24, January 1969

5. Townsend, A.A., <u>The Structure of Turbulent Shear Flow</u>, Cambridge University Press, Cambridge, England 1956

6. Demetriades, A., <u>Mean-Flow Measurements in an Axisymmetric Compressible Turbulent Wake</u>, AIAA J. Vol. 6, No. 3, p 432, March 1968

7. Demetriades, A., <u>Hot Wire Measurements in the Hypersonic Wakes of Slender Bodies</u>, AIAA J. Vol. 2, No. 2, p 245, February 1964

8. Demetriades, A., and Gold, H., <u>Transition to Turbulence in the Hypersonic Wakes of Blunt-Bluff Bodies</u>, ARS J., Vol. 32, No. 9, p 1420, September 1962

9. Ames Research Staff, <u>Equations, Tables and Charts for Compressible Flow</u>, NACA TR 1135, Washington, D.C., 1953. See, also, Mueller, J.N., <u>Equations, Tables and Figures for Use in the Analysis of Helium Flow at Supersonic and Hypersonic Speeds</u>, NACA TN 4063, Washington, D.C., 1957

10. Dewey, Jr., C.F., <u>Private Communications</u>, California Institute of Technology, Pasadena, California, 1960-1962

TABLE I

TABLE OF PHYSICAL COORDINATES OF CUSP NOZZLES

ξ (in.)	χ (in.)	ξ (in.)	χ (in.)
0	.5142		
.0398	.4896	.1808	.4089
.052	.482	.1916	.4034
.0575	.4784	.2029	.3978
.0618	.4759	.2153	.3918
.0646	.4741	.2272	.3862
.0674	.4726	.2398	.3803
.0699	.4711	.2530	.3744
.0734	.469	.2658	.3686
.0836	.4627	.2945	.3563
.0873	.4603	.3251	.3437
.0912	.4579	.3582	.3307
.0943	.4562	.394	.3172
.0971	.4545	.4326	.3034
.100	.4527	.4748	.2889
.1025	.4511	.5215	.2742
.1074	.449	.5715	.2592
.1125	.4463	.6274	.2433
.117	.4436	.6866	.2274
.1214	.4407	.7525	.2111
.1268	.4376	.904	.1768
.137	.432	1.0888	.141
.146	.427	1.3161	.1045
.1529	.4235	1.5902	.0704
.1616	.4189	1.9317	.0407
.1704	.4143	2.3479	.0176
		2.6157	.0076
		2.8545	.005

36
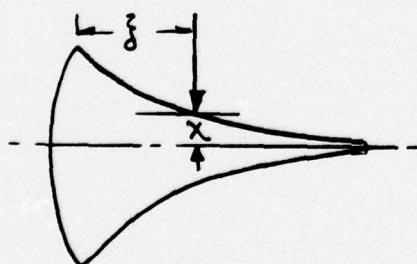
TABLE II

COEFFICIENTS C_n

n= \ Degree	4	5	6	7	8
1	7.854531	10.62409	13.90497	16.69116	19.3553
2	-24.88887	-51.14484	-98.28814	-156.8195	-233.4886
3	31.898	112.3132	335.6014	750.3165	1499.482
4	-13.97012	-111.6295	-572.6051	-1910.121	-5325.4
5	-	40.77446	471.7772	2632.214	10866.19
6	-	-	-149.4286	-1851.714	-12672.24
7	-	-	-	520.4112	7838.28
8	-	-	-	-	-1991.188

TABLE III

Values of $F(M_\infty, \gamma)$ for Various Values of M_∞, γ (Laminar Viscous Force Calculation)

γ \ M_∞	2	3	4	5	6
1.2	1.199222	1.977851	4.011097	8.443294	17.32144
1.3	1.316166	2.099284	3.830711	6.982828	12.22896
1.4	1.4322	2.231281	3.804024	6.361286	10.17771
1.5	1.547565	2.369352	3.852264	6.082258	9.178528
1.6	1.662436	2.511236	3.942517	5.974535	8.654355
1.667	1.739188	2.607782	4.018111	5.959569	8.451732

37

TABLE IV

Values of the Integral i for Various Values of M_∞ and γ (Laminar Shear Force on Nozzle)

γ \ M_∞	2	3	4	5	6
1.2	1.628	1.238	.8422	.5827	.4257
1.25	1.559	1.192	.8283	.5861	.4346
1.3	1.496	1.148	.8121	.5855	.4401
1.35	1.438	1.107	.7947	.5819	.4427
1.4	1.384	1.068	.7766	.5763	.4432
1.45	1.335	1.032	.7584	.5692	.4419
1.5	1.289	.9985	.7403	.5612	.4393
1.55	1.246	.9667	.7224	.5524	.4357
1.6	1.206	.9368	.705	.5431	.4313
1.65	1.168	.9087	.688	.5337	.4263
1.667	1.156	.8995	.6823	.5304	.4245

TABLE V

Values of the Non-Dimensional Parameter $\mathcal{F}$ (M_∞, γ) (Laminar Viscous Force Calculation)

γ \ M_∞	2	3	4	5	6
1.2	3.124	4.653	7.092	11.28	18.21
1.3	3.148	4.579	6.532	9.371	13.29
1.4	3.169	4.528	6.202	8.402	11.14
1.5	3.188	4.495	5.987	7.824	9.959
1.6	3.205	4.47	5.835	7.437	9.219
1.667	3.214	4.456	5.756	7.245	8.861

TABLE VI

Values of the Parameter $i'(M_\infty\infty, \gamma)$
(Laminar Nozzle Heat Transfer Calculation)

γ \ M_∞	2	3	4	5	6
1.2	1.102	.706	.4505	.3063	.2235
1.3	1.069	.7056	.4705	.3317	.2473
1.4	1.04	.701	.4826	.3498	.266
1.5	1.012	.694	.4894	.3626	.2804
1.6	.9864	.6856	.4927	.3713	.2913
1.667	.9702	.6795	.4935	.3755	.297

TABLE VII

Heating/Cooling Efficiency $Q/\alpha = S(M\infty, \gamma)$
(Laminar Nozzle Heat Transfer Calculation)
(assuming $\sigma = 0.75$)

γ \ M_∞	2	3	4	5	6
1.2	10.58911	10.47221	7.742076	5.201797	3.407888
1.3	3.810589	2.838522	1.843574	1.181419	.7736683
1.4	2.069132	1.353306	.8382526	.532963	.3529183
1.5	1.345312	.8203605	.4981618	.3174406	.2127716
1.6	.9691441	.565502	.3403711	.2178862	.1476262
1.667	.8067598	.4611308	.2768253	.1778572	.1212345

TABLE VIII

Values of the Parameter i" (M_∞, γ)
(Turbulent Nozzle Friction Calculation)

γ \ M_∞	2	3	4	5	6
1.2	0.6617	.324	.1435	.07301	.04469
1.3	.6022	.3078	.1474	.0787	.04824
1.4	.5508	.2897	.1465	.08151	.05072
1.5	.506	.2715	.1429	.08217	.05205
1.6	.4669	.254	.1379	.08138	.05243
1.667	.4433	.243	.134	.08031	.05227

TABLE IX

Values of the Parameter N (M_∞, γ)
(Turbulent Nozzle Friction Calculation)

γ \ M_∞	2	3	4	5	6
1.2	1.655105	3.960981	12.3285	39.64081	121.0351
1.3	1.721604	3.623439	8.950495	21.74909	49.5111
1.4	1.789865	3.436148	7.312879	15.02337	28.91889
1.5	1.859242	3.330792	6.387842	11.73384	20.26371
1.6	1.929334	3.274796	5.815821	9.862627	15.78614
1.667	1.976565	3.255865	5.549056	9.024275	13.88738

TABLE X

Values of the Parameter $G (M_\infty, \gamma)$
(Turbulent Nozzle Friction Calculation)

γ \\ M_∞	2	3	4	5	6
1.2	.06909	.09623	.1466	.2618	.5272
1.3	.06542	.0836	.1093	.1548	.2328
1.4	.0622	.07464	.08876	.1107	.143
1.5	.05934	.06779	.07561	.08717	.1028
1.6	.05682	.06238	.06644	.07259	.08069
1.667	.05526	.05933	.0616	.06554	.07076

TABLE XI

Heating/Cooling Efficiency $Q/_\alpha$
(Turbulent Nozzle Heat Transfer Calculation)

γ \\ M_∞	2	3	4	5	6
1.2	1.882194	1.211807	1.016553	.9570714	.9236017
1.3	1.42432	.9746492	.8367381	.7888347	.7648494
1.4	1.193997	.8557685	.749112	.708328	.6872611
1.5	1.056738	.7847835	.697265	.6619956	.6431093
1.6	.8855203	.738219	.6628954	.6317148	.6148905
1.667	.9179515	.7141839	.6463789	.6170509	.600834

41

TABLE XII

Values of the Parameter $i'''(M_\infty, \gamma)$
(Turbulent Nozzle Heat Transfer Calculation)

γ \ M_∞	2	3	4	5	6
1.2	.421	.1709	.07238	.03735	.02309
1.3	.407	.1761	.08028	.04273	.02625
1.4	.3924	.1778	.08568	.04713	.02922
1.5	.3781	.1773	.08912	.05048	.03175
1.6	.3344	.1754	.0911	.0529	.03378
1.667	.3555	.1736	.09181	.05408	.03487

TABLE XIII

Values of the Parameter $K(M_\infty, \gamma, Re_{h_1})$
(Turbulent Wake Thickness Calculation)

γ \ M_∞	2	3	4	5	6
1.2	.5391567	.6770355	.8655276	1.193497	1.739235
1.3	.5245009	.6311099	.7473666	.9178681	1.155874
1.4	.5115746	.5962623	.6735038	.7762537	.905835
1.5	.4996897	.5683407	.6216873	.6887616	.7680517
1.6	.4889489	.5450785	.5827305	.6285309	.6805207
1.667	.4822006	.5317594	.5610909	.5972383	.6372909

TABLE XIV

Values of the Length-to-Exit Height Ratio
for GDL Nozzles

M	$\dfrac{\ell}{h_1}$	$\sqrt{\dfrac{\ell}{h_1}}$
2	1.45	1.204
3	2.05	1.431
4	2.5	1.581
5	2.98	1.726
6	3.46	1.86

43
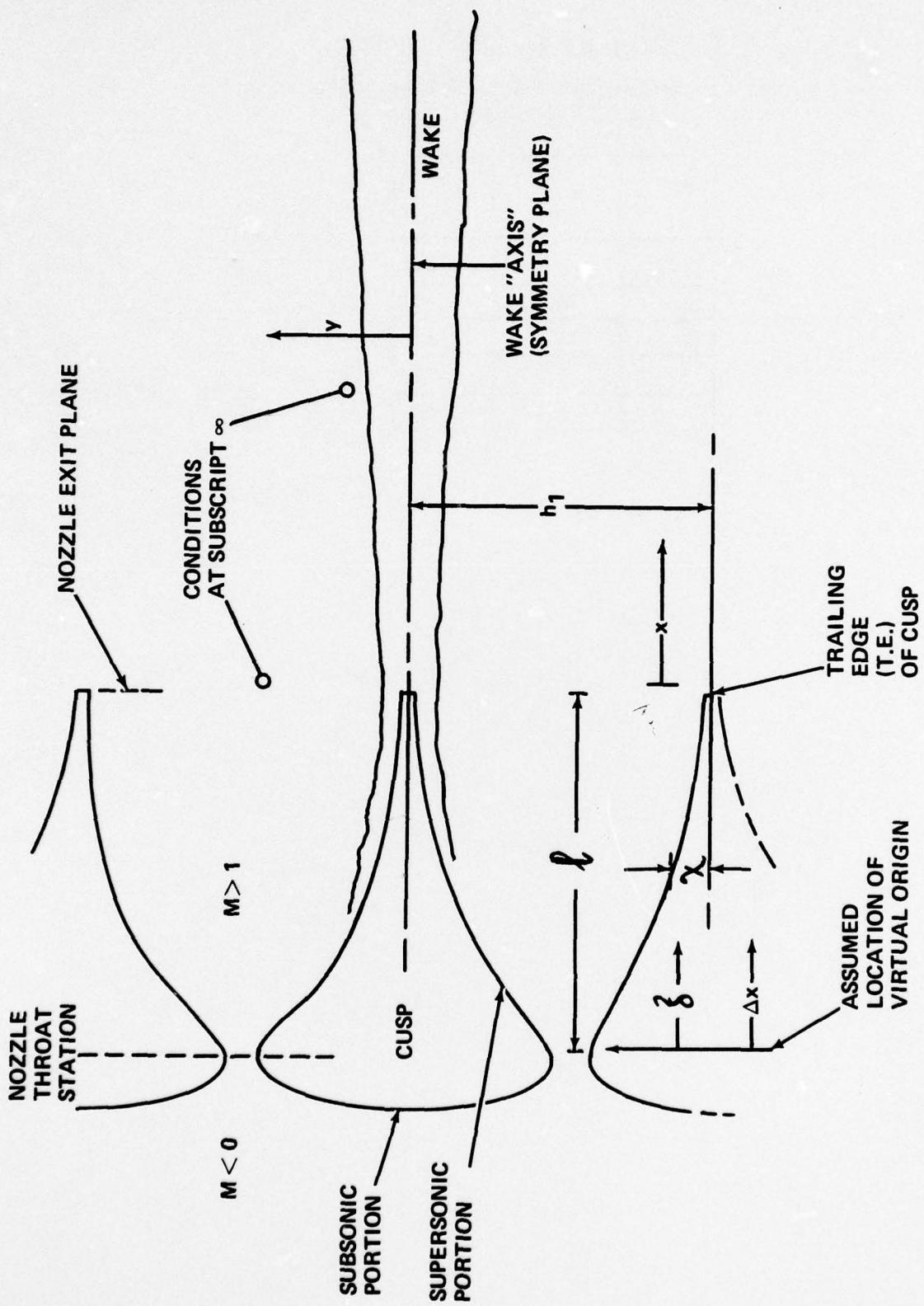
FIGURE 1. Schematic of nozzle-cusp geometry showing nomenclature

44

$\gamma = 1.4, M = 4$

$$\int_{o}^{1} \sqrt{\frac{\frac{z}{\xi}}{\frac{z}{\xi}}} M^{3/2} \left(1 + \frac{M^2}{5}\right)^{-2} \left(1 + \frac{\gamma - 1}{2} M^2\right)^{-0.38} d\left(\frac{z}{\ell}\right)$$

POLYNOMIAL DEGREE ⟶

POLYNOMIAL FIT:

○ 4TH DEGREE
△ 5TH DEGREE
□ 6TH DEGREE
✕ 7TH DEGREE
● 8TH DEGREE

$\frac{z}{\ell}$

Z
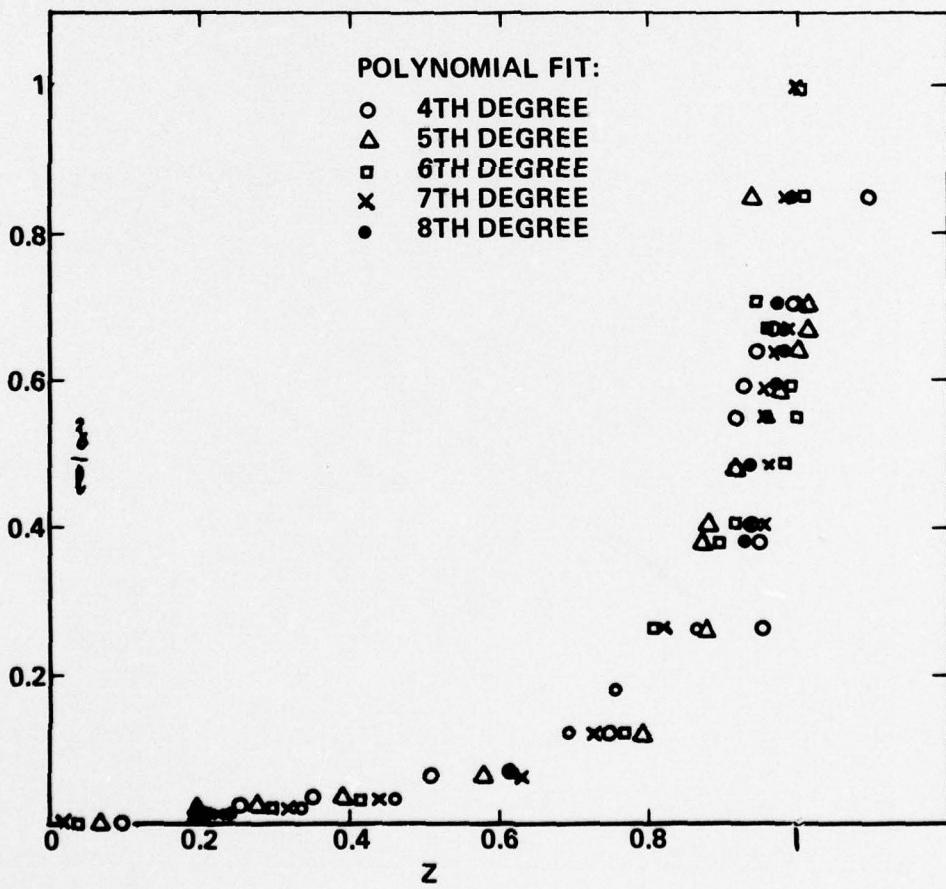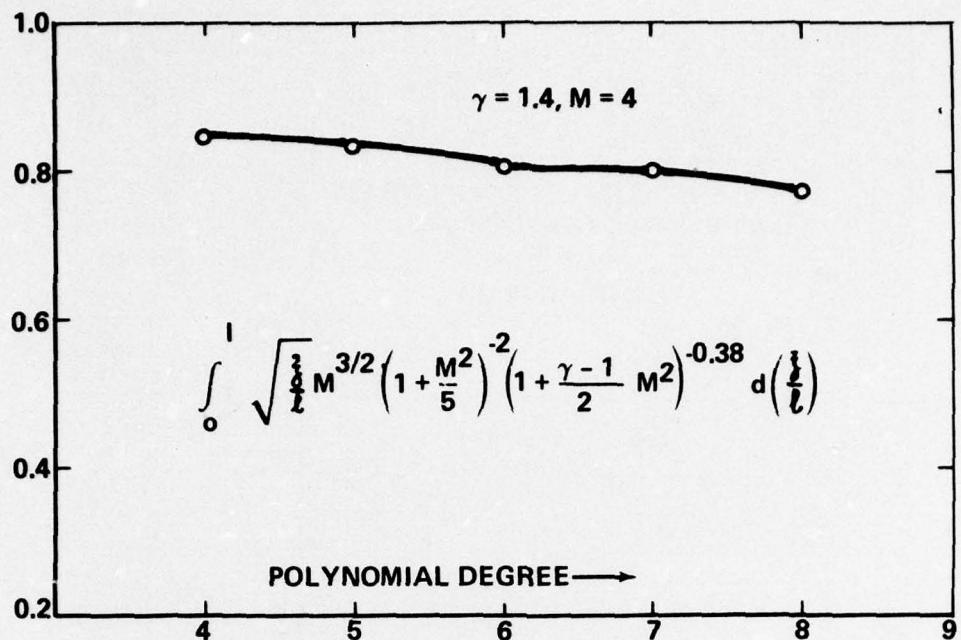
FIGURE 2. The function z(M) for the GDL nozzles
considered herein

45
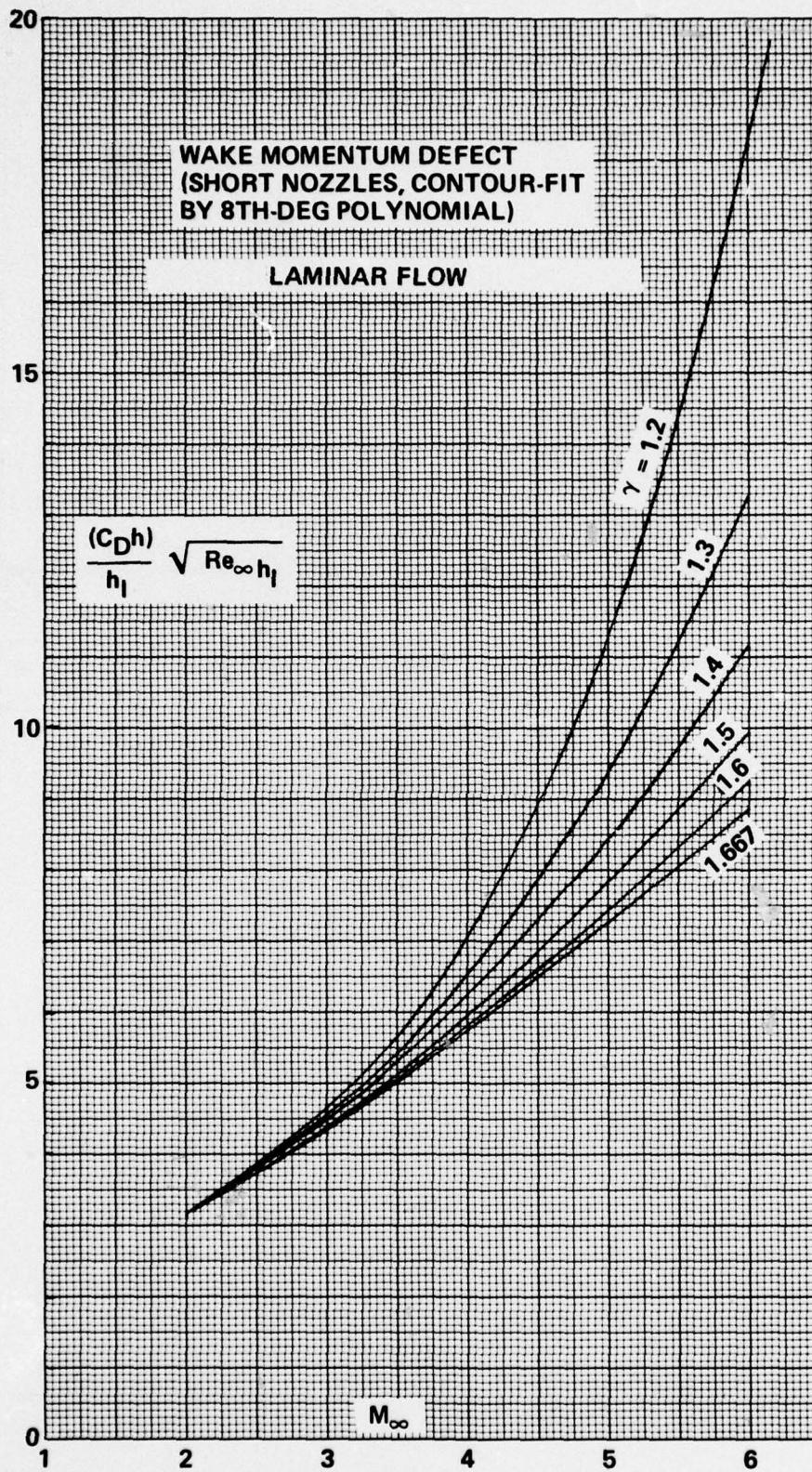
FIGURE 3. The function $\mathcal{F}$ indicative of the total cusp drag in laminar flow

46
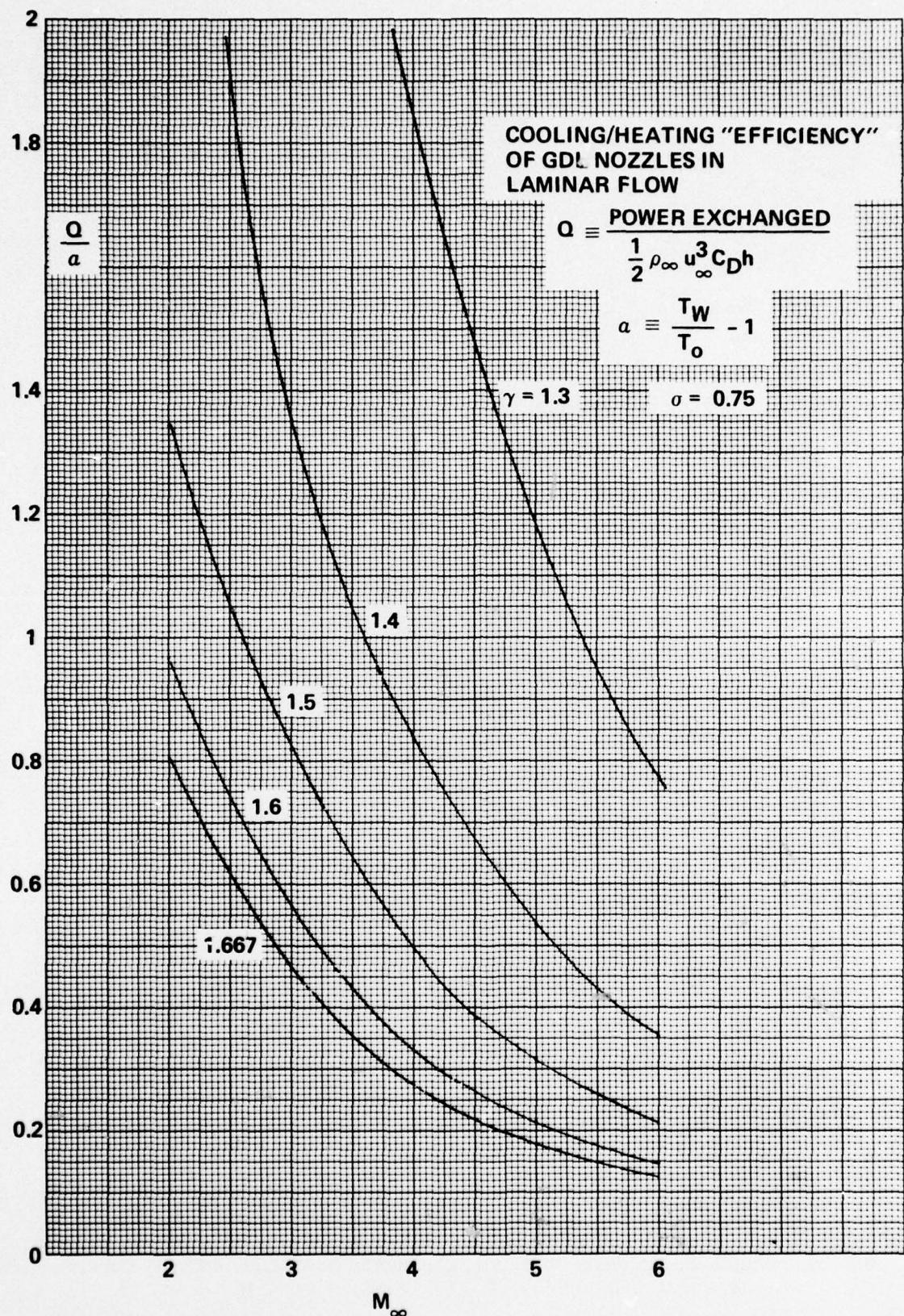
FIGURE 4. The function S indicative of the ease with
which heat is exchanged between cusp and
laminar nozzle flow

47
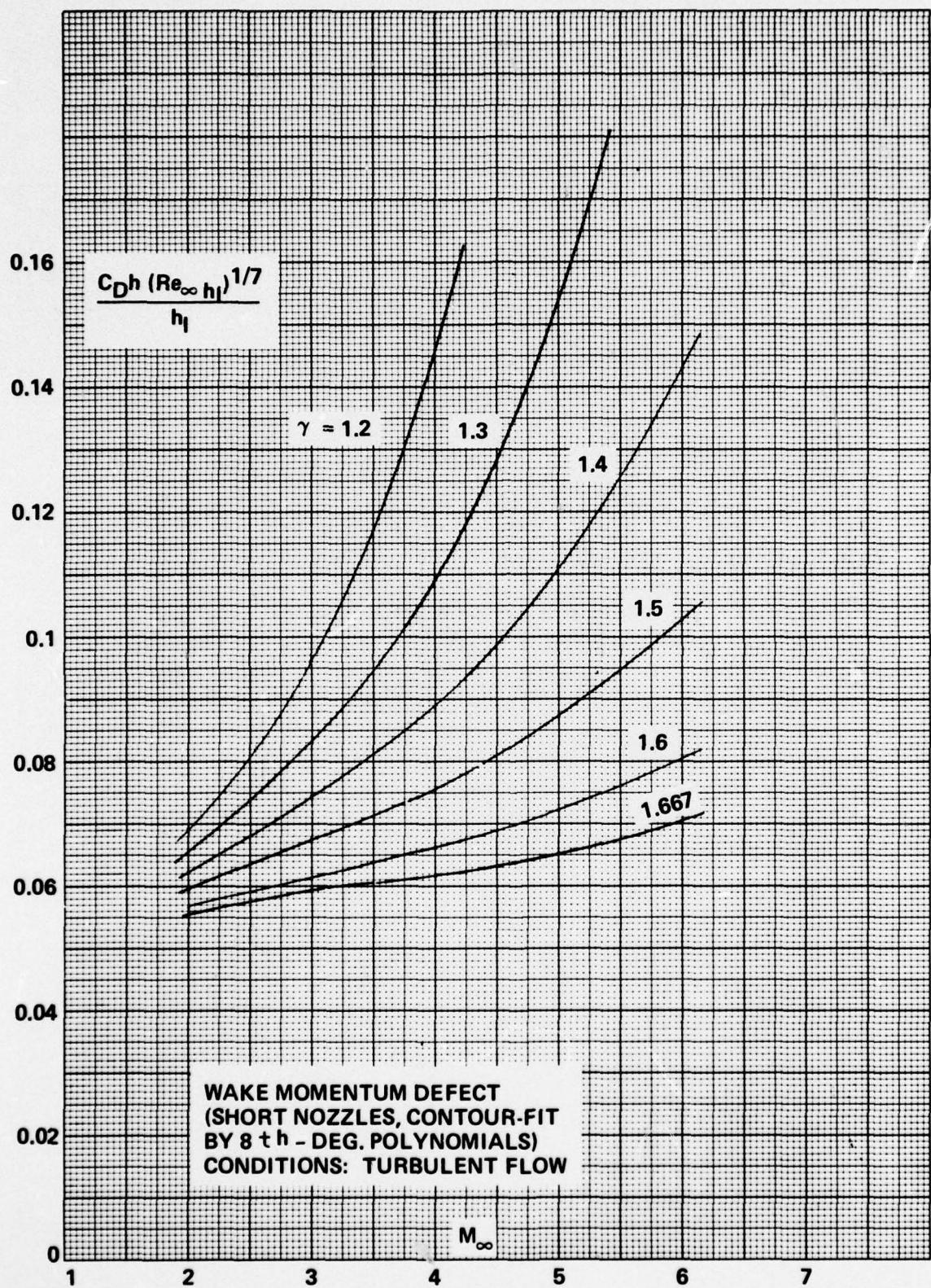
FIGURE 5. The function G indicative of the total cusp
drag in turbulent flow

48
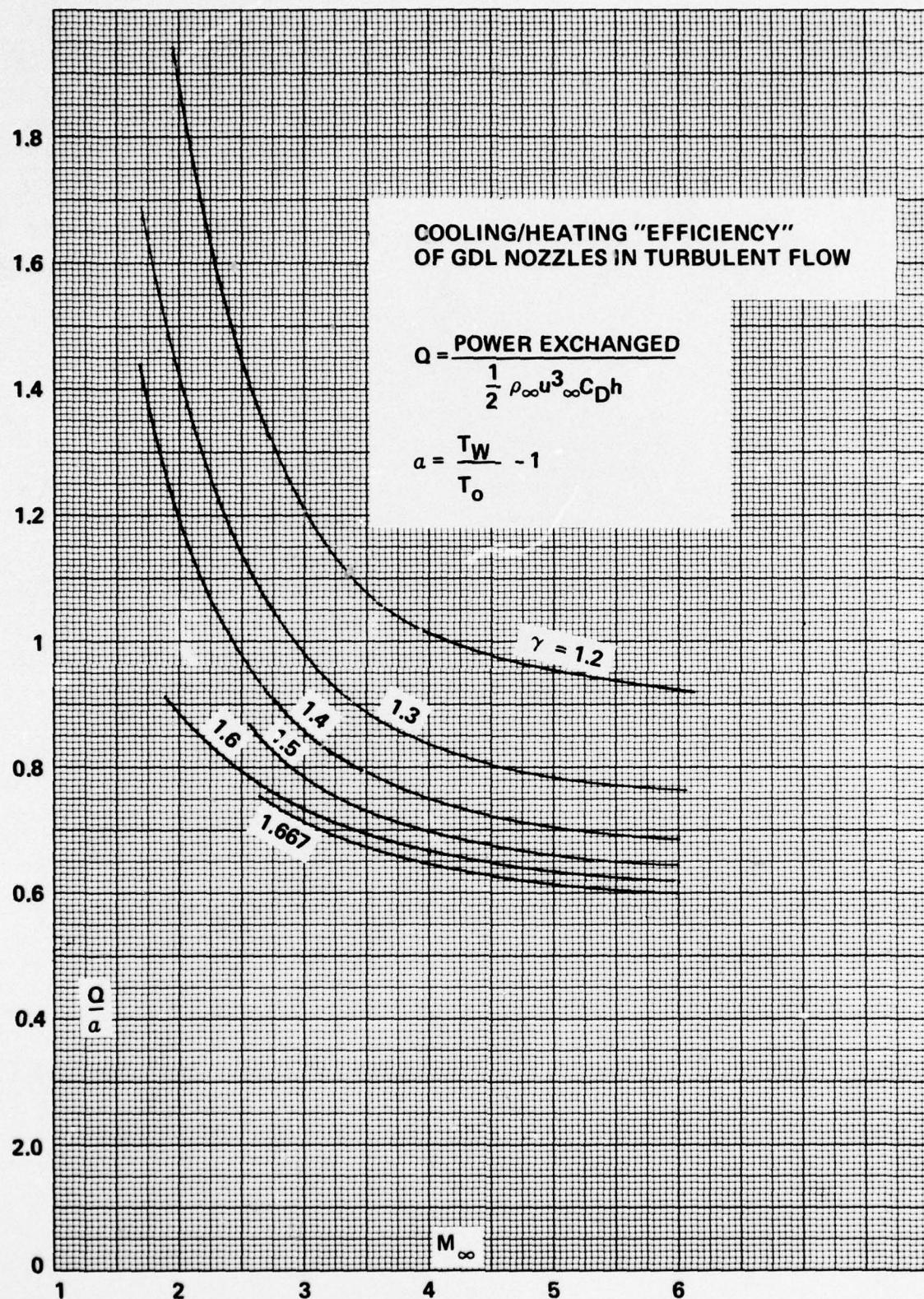
FIGURE 6. The function Q/α indicative of the ease with which heat is exchanged between cusp and turbulent nozzle flow

49
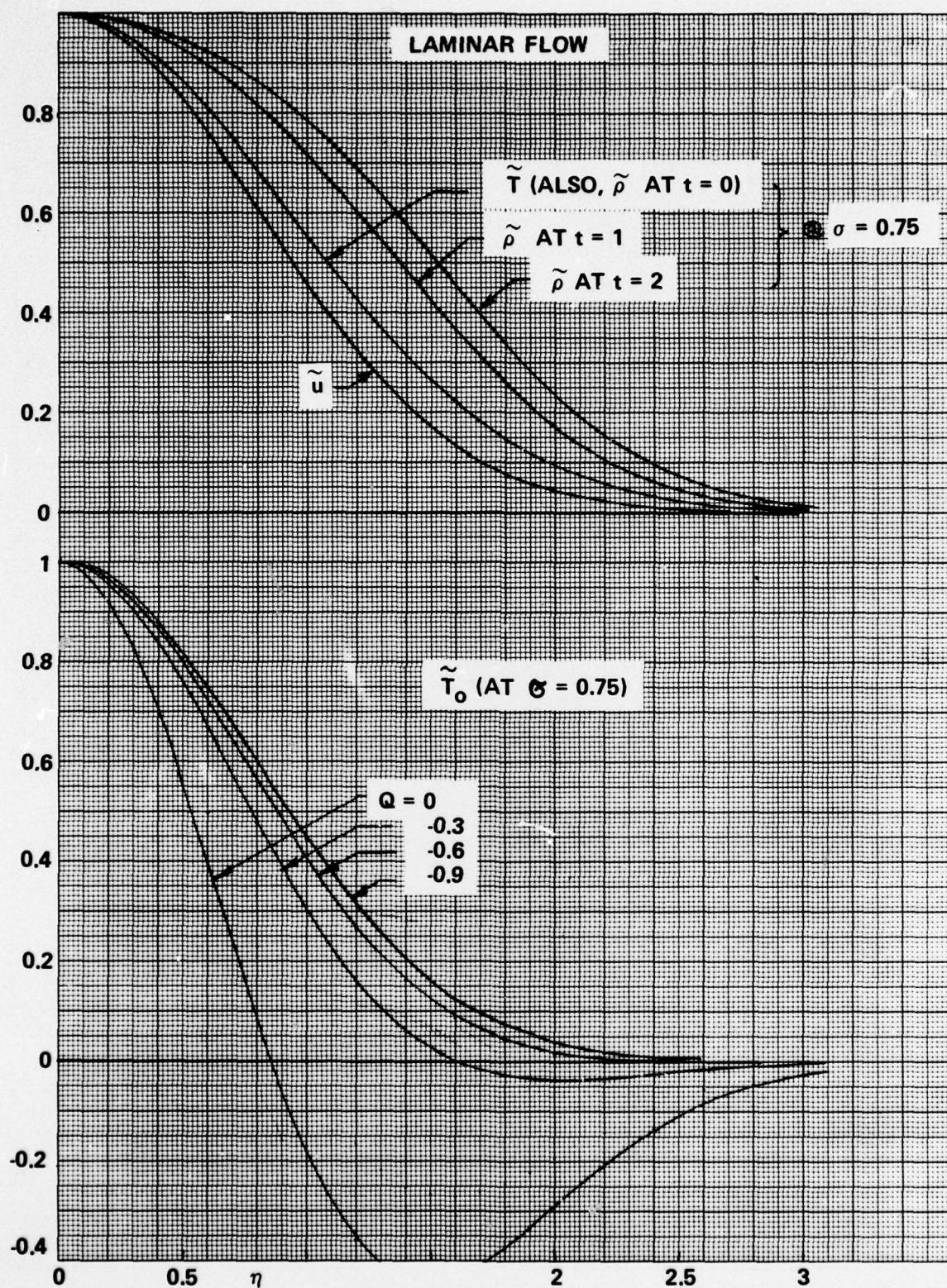
FIGURE 7a. Laminar lateral profiles

50
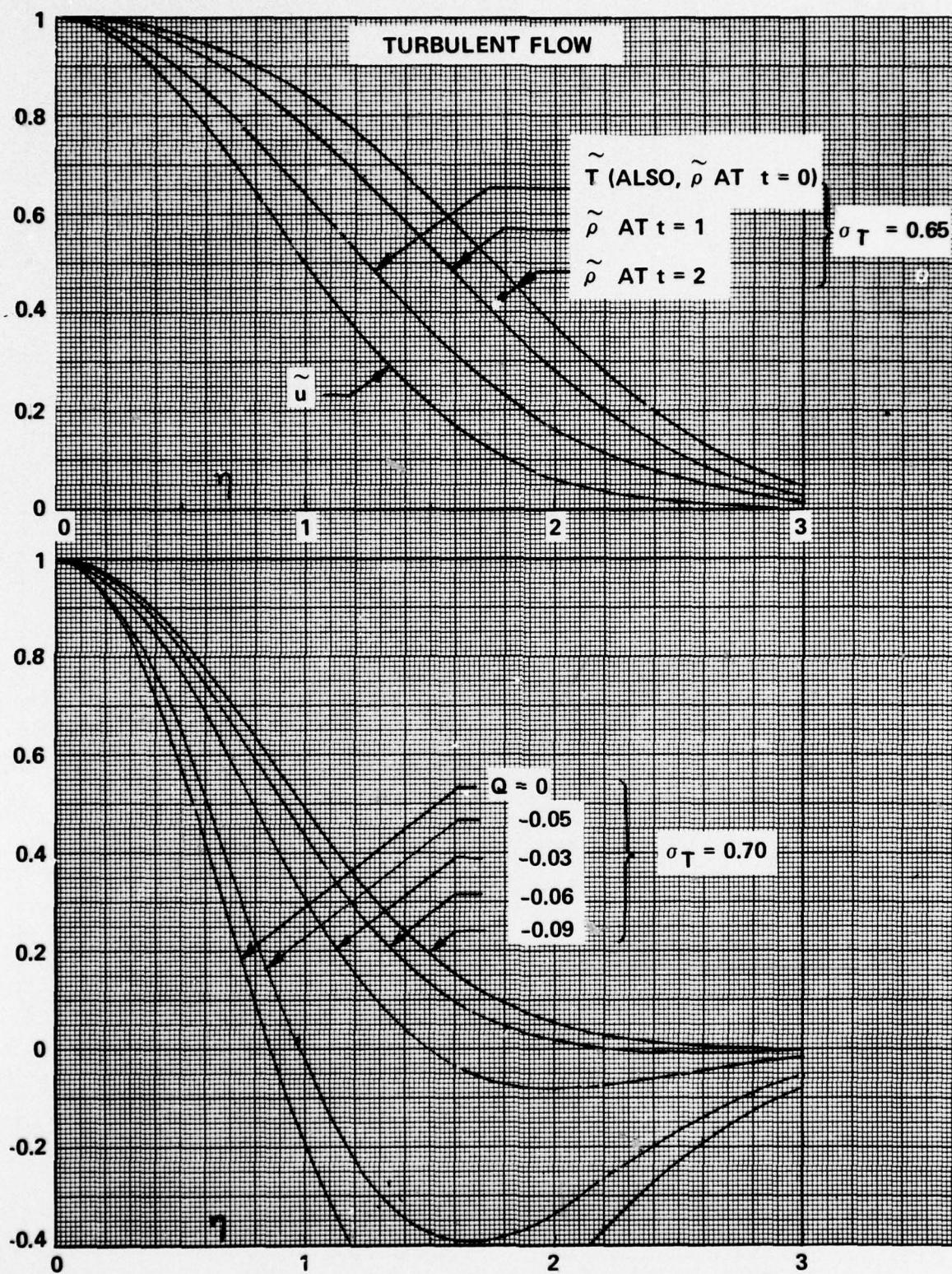
FIGURE 7b. Turbulent lateral profiles

51
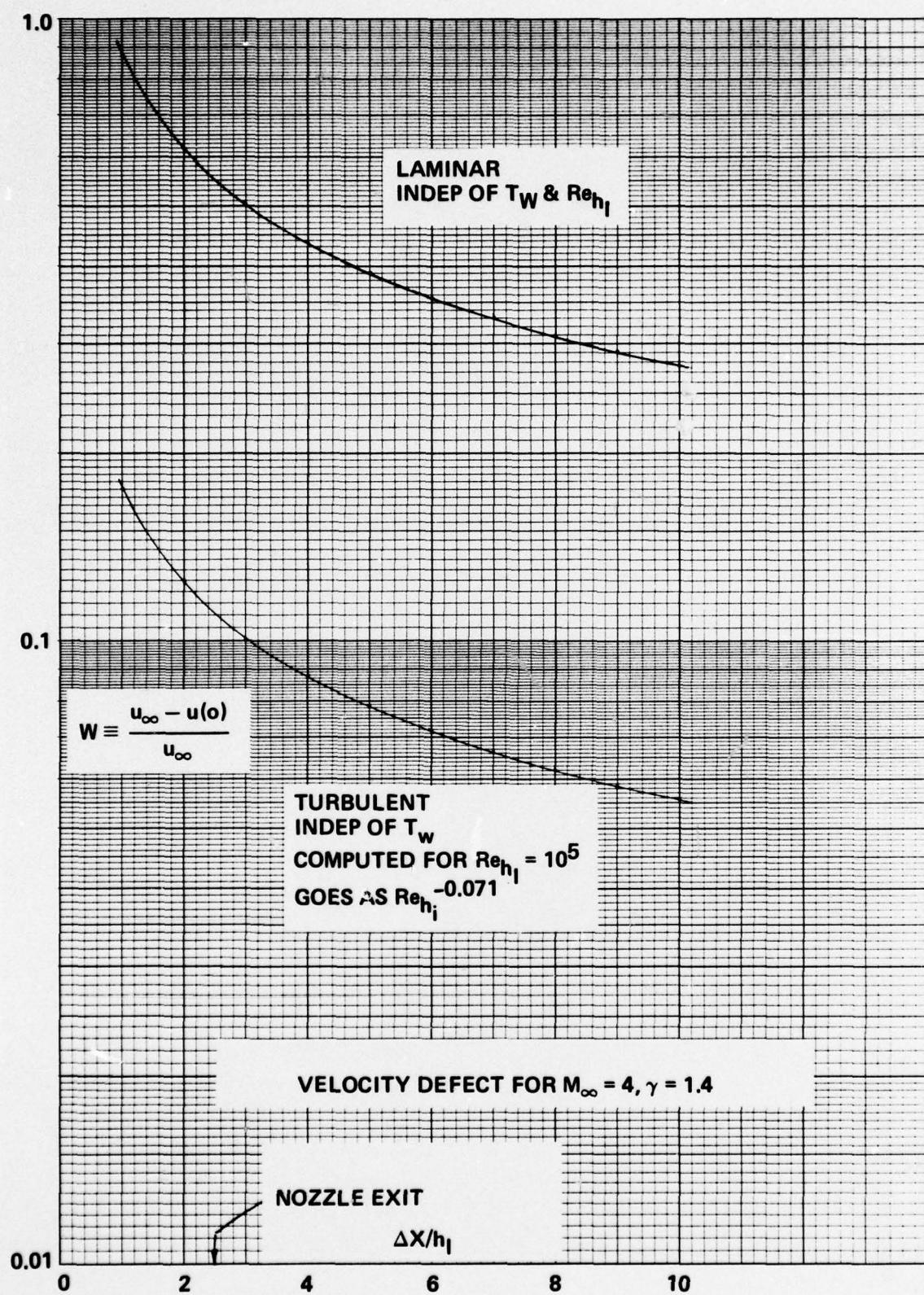
FIGURE 8. Velocity defect for $M_\infty = 4$, $\gamma = 1.4$

52
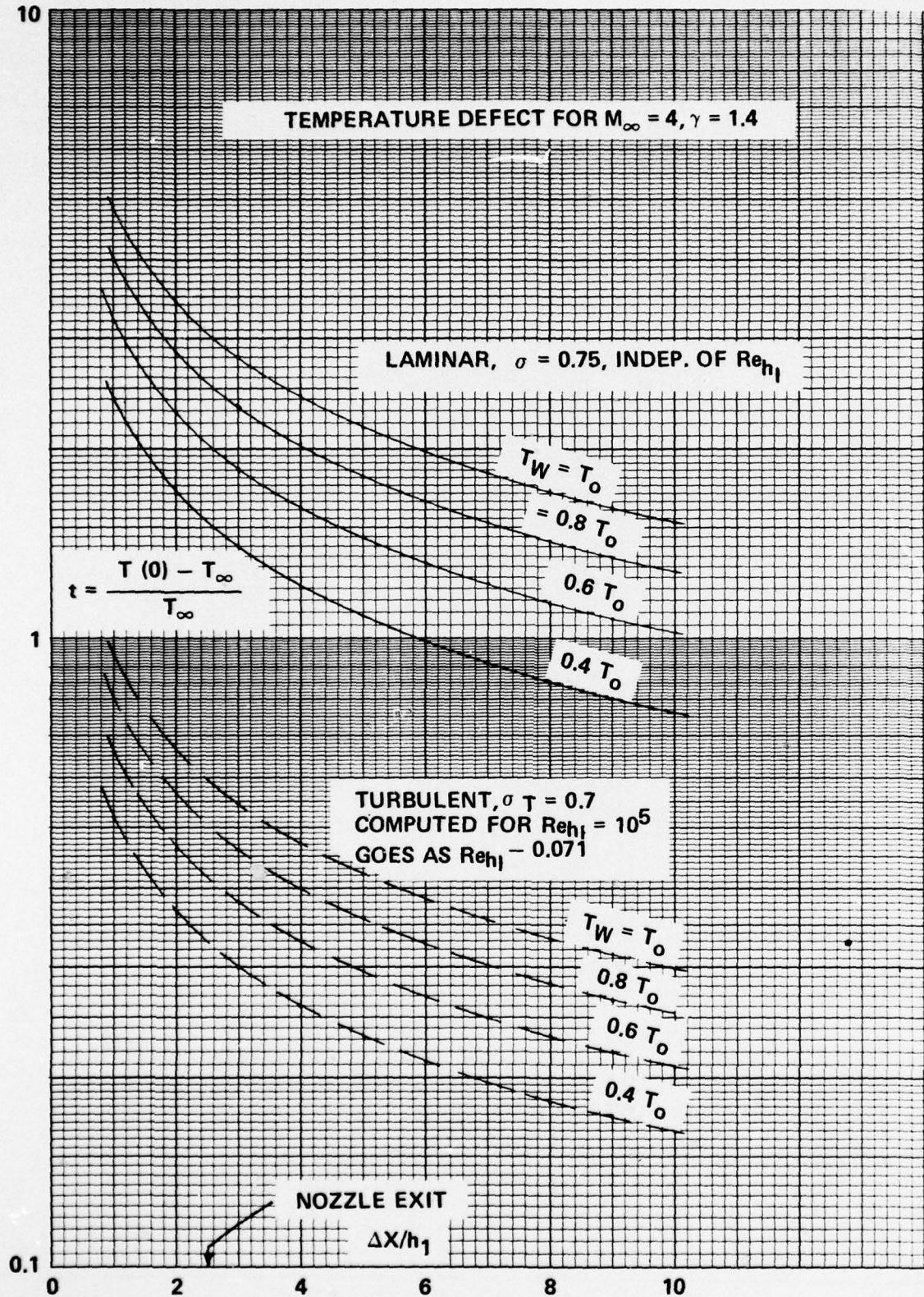
FIGURE 9. Temperature defect for $M_\infty = 4$, $\gamma = 1.4$

53
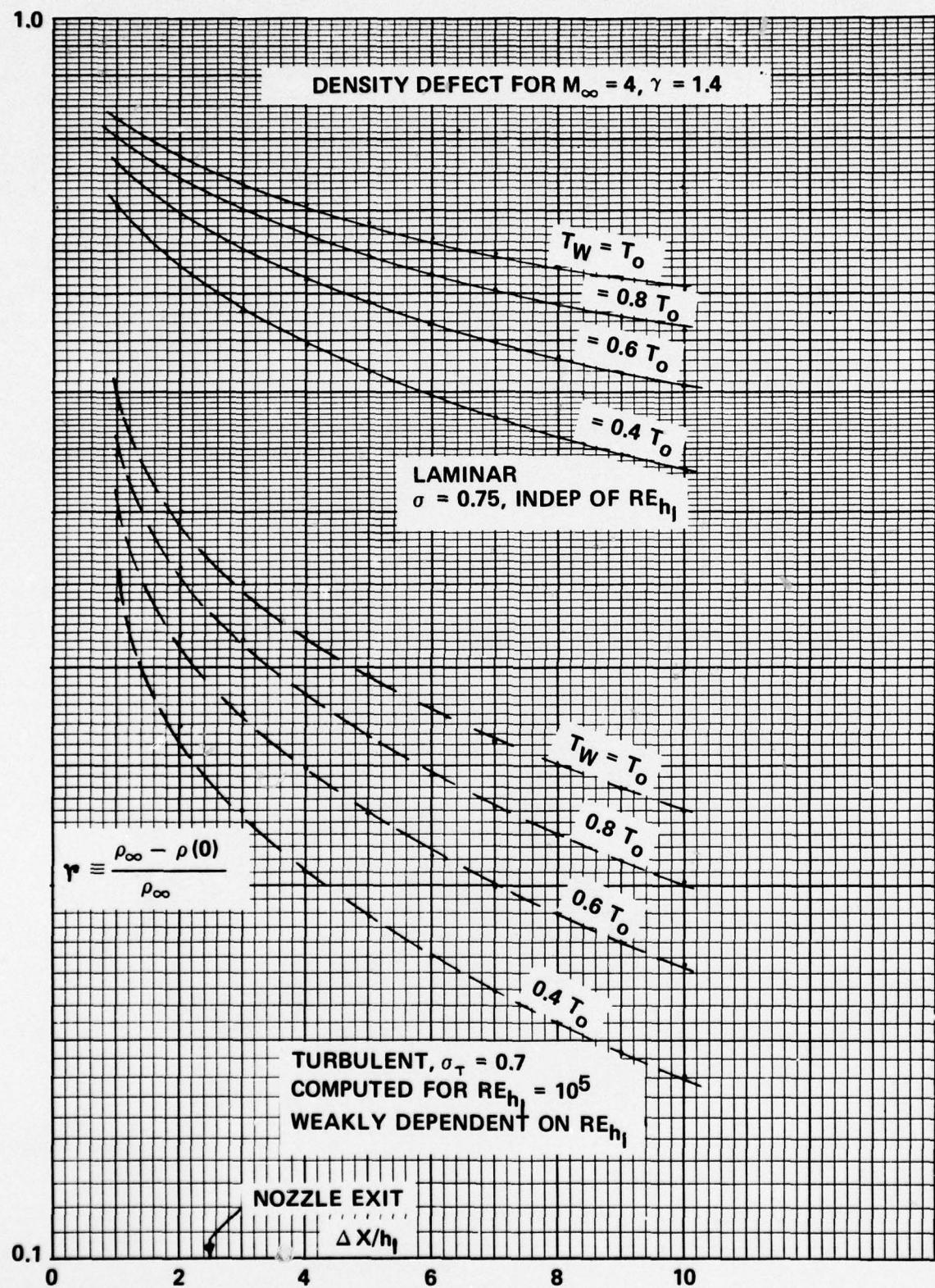
FIGURE 10. Density defect for $M_\infty = 4$, $\gamma = 1.4$

54
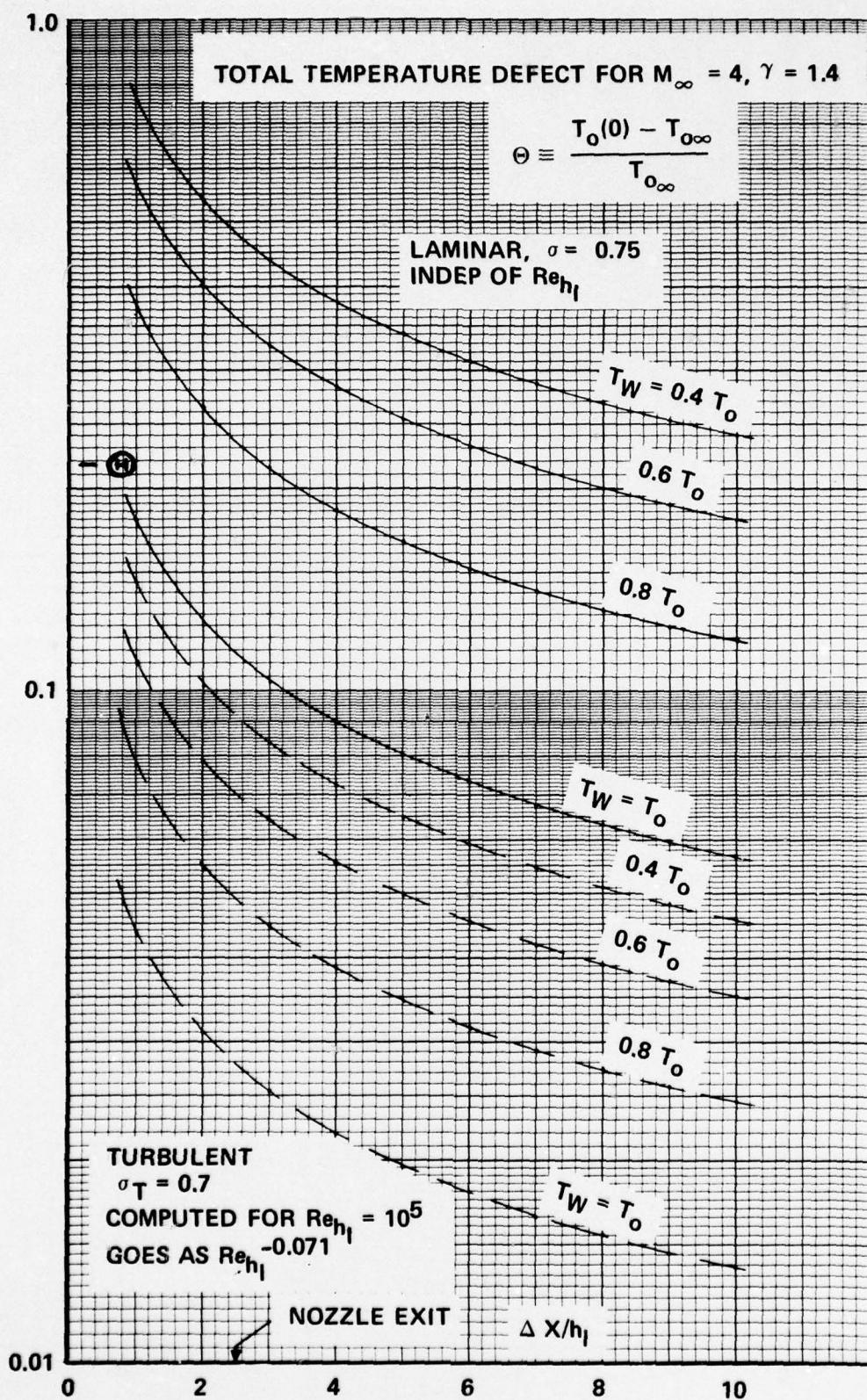
FIGURE 11. Total temperature defect for $M_\infty = 4$, $\gamma = 1.4$

55
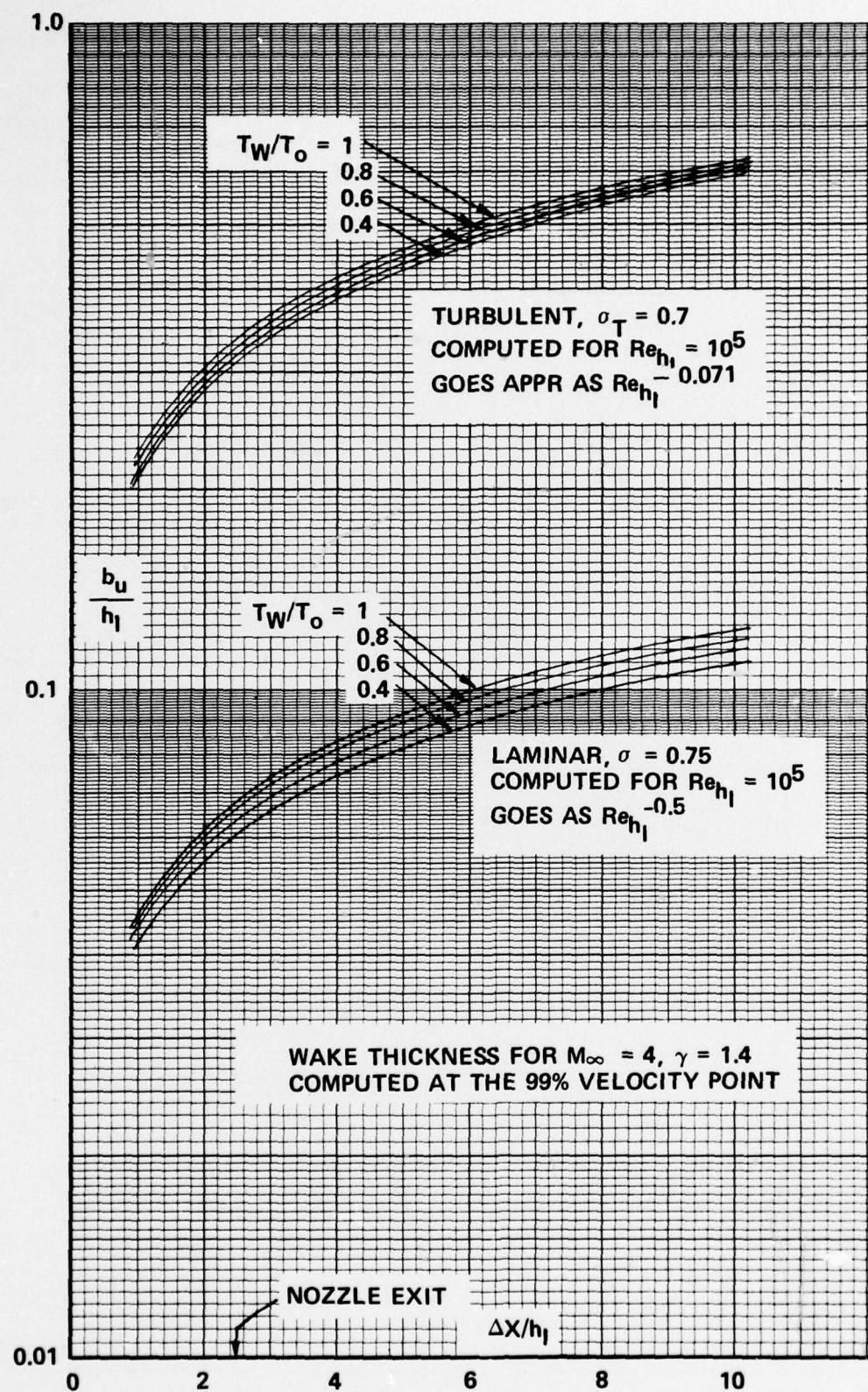
FIGURE 12. Wake thickness for $M_\infty = 4$, $\gamma = 1.4$

56